To the Graduate Council:

I am submitting herewith a thesis written by Xiaohang Peng entitled "Sensitivity Study of the Effects of PDF Models on the Predicted Structure of Turbulent Combustor Flow." I have examined the final copy of this thesis for form and content and recommend that it be accepted in partial fulfillment of the requirements for the degree of Master of Science, with a major in Mechanical Engineering.

Roy J. Schulz

Roy J. Schulz, Major Professor

We have read this thesis
and recommend its acceptance:

Hayden Crawford

Walter Frost

Accepted for the Council:

C W Minkel

Vice Provost
and Dean of the Graduate School

SENSITIVITY STUDY OF THE EFFECTS OF PDF MODELS ON THE PREDICTED STRUCTURE OF TURBULENT COMBUSTOR FLOW

A Thesis

Presented for the

Master of Science

Degree

The University of Tennessee, Knoxville

Xiaohang Peng

August 1988

ACKNOWLEDGMENTS

The work reported herein was supported by the U.S. Department of Energy under contract No. DE-AC02-79ET10815 at the University of Tennessee Space Institute, Tullahoma, TN 37388.

The author wishes to express his sincere appreciation to Dr. Roy J. Schulz, for his suggesting this topic and for his guidance and invaluable help throughout the course of this study and investigation.

The author is indebted to his committee Dr. Lloyd W. Crawford and Dr. Walter Frost, for their careful review this thesis and helpful comments.

Special gratitude to Dr. Ying-Chu L. Susan Wu, for her special advice and encouragement.

Finally, but by no means least, the author would like to thank his wife, Quan, for her patient, love, and assistance.

ABSTRACT

A series of numerical calculations was made of a specified, turbulent, recirculating flow in a cylindrical combustor operating with a methane-air, non-premixed diffusion flame. For all calculations, the same fuel to air mean flow ratio was used, so the overall stoichiometry of the flame was fixed. The calculations were done with three different fuel and air jet inlet velocities, and three different fuel jet turbulence levels, determined by the magnitude of the input kinetic energy profiles of the fuel jet. The flows were calculated with three ways to obtain the mean temperature, molecular weight and density distributions: without using a probability density function (pdf), with a Clipped-Gaussian pdf, and with a two-delta function pdf. The purpose of the calculations was to determined the variation between different calculated flows, with and without pdf applications, and how sensitive the computed flow field structure was to inlet velocity (Reynolds number) effects and inlet turbulence (fluctuation level) effects. The results justify the use of the computationally more expensive pdf approach (the Clipped-Gaussian) to compute such flows.

TABLE OF CONTENTS

CHAPTER PAGE

I. INTRODUCTION 1

1.1. Background 1

1.2. Objective of Present Study 3

II. PDF MODELS FOR TURBULENT DIFFUSION FLAMES 5

2.1. Determination and Use of PDF'S 5

2.2. Thermal Equation of State 7

2.2.1. Combustion Chemistry 7

2.2.2. Flame Sheet Model 8

2.2.3. Temperature,Density and Molecular Weight Functions . . . 10

2.3. PDF Models 12

2.4. Density Dependent Solution Behavior 15

III. PREDICTION TECHNIQUES 18

3.1. Governing Equations 18

3.2. Boundary Conditions 21

3.2.1. Fuel Fraction and its Variance 21

3.2.2. Inlet Conditions for u, v, k, ϵ, and μ_E 22

3.3. Solution Techniques and Finite Difference Formulation 25

IV. RESULTS AND ANALYSIS 27

4.1. The Cases Evaluated 27

4.2. Results of The Comparisons 29

4.2.1. Streamlines Patterns and Recirculation Zones 29

4.2.2. Profiles of Mean Scalar Quantities 39

V. SUMMARY AND CONCLUSIONS 47

5.1. Summary 47

5.2. Conclusions 47

LIST OF REFERENCES 49

APPENDIXES 53

APPENDIX A. DERIVATION OF 2-DELTA FUNCTION PDF . . . 54

APPENDIX B. INLET CONDITION FOR MEAN AXIAL VELOCITY 57

VITA 59

LIST OF FIGURES

FIGURE PAGE

1. Schematic of "Over-Ventilated" Diffusion Flame in Combustor 2
2. Schematic and Dimensions of Modeled Combustor 4
3. Relation between f and Scalar Properties 11
4. Variation of Density with f 16
5. Comparison of Recirculation Zone Structure Obtained with No-PDF, 2-δ Functions PDF, and Clipped-Gaussian PDF for 7 m/s Fuel Mean Velocity, 1% Inlet Fuel Stream Turbulence 30
6. Comparison of Recirculation Zone Structure Obtained with No-PDF, 2-δ Functions PDF, and Clipped-Gaussian PDF for 25 m/s Fuel Mean Velocity, 1%Inlet Fuel Stream Turbulence 31
7. Comparison of Recirculation Zone Structure Obtained with No-PDF, 2-δ Functions PDF, and Clipped-Gaussian PDF for 86 m/s Fuel Mean Velocity, 1%Inlet Fuel Stream Turbulence 32
8. Comparison of Recirculation Zone Structure for Changes in Fuel Mean Velocity (7& 25 m/s), 1%Inlet Fuel Stream Turbulence 33
9. Comparison of Recirculation Zone Structure for Changes in Fuel Mean Velocity (7& 86 m/s), 1%Inlet Fuel Stream Turbulence 34
10. Comparison of Recirculation Zone Structure Obtained with No-PDF, 2-δ Functions PDF, and Clipped-Gaussian PDF for 5% Fuel Turbulence Intensity, 7m/s Inlet Fuel Mean Velocity 36
11. Comparison of Recirculation Zone Structure for Changes in Turbulence Intensity (1% & 5%), 7m/sec Inlet Fuel Mean Velocity 37

12. Comparison of Recirculation Zone Structure for Changes in Turbulence Intensity (1% & 25%), 7m/sec Inlet Fuel Mean Velocity 38
13. Comparison of Predicted Mean Axial Velocity Profiles Across Combustor 40
14. Comparison of Predicted Mean Temperature Profiles Across Combustor 41
15. Comparison of Predicted Mean Density Profiles Across Combustor 42
16. Comparison of Predicted Mean Turbulent Kinetic Energy Profiles Across Combustor 43
17. Comparison of Predicted Mean Turbulent Effective Viscosity Profiles Across Combustor 44

LIST OF TABLES

TABLE PAGE

1. Source Terms and Exchange Coefficients Used in the General Equation of ϕ 19
2. Combustion Model Constants 20
3. The Form of the Components of the Linearized Source Term 26
4. The Cases Evaluated 27

LIST OF SYMBOLS

$\tilde{a}_j$	coupling coefficient for some cell face
A	Integral constant defined in eq. (2.32)
A^+	Experimental constant
B	Integral constant defined in eq. (2.32)
C_1	Constant of turbulence model
C_2	Constant of turbulence model
C_D	Constant of turbulence model
C_{g_1}	Constant of turbulence model
C_{g_2}	Constant of turbulence model
c_p	constant-pressure specific heat
D	diameter of circular jet (0.5 inches)
f	Mixture mass fraction
f_{stoich}	Stoichiometric mixture mass fraction
$\bar{f}$	Time or ensembling average mixture mass fraction
f_-, f_+	Components of two-delta functions pdf
g	Variance of $\bar{f}$
G	Defined in eq. (3.7)
h	Enthalpy
H_F	Heat of combustion of fuel
i	The fuel to air mass ratio
k	Turbulence kinetic energy
l	Mixing length
L	Length of combustor
m_A	Mass fraction of air

m_{A_0}	Inlet mass fraction of air
m_F	Mass fraction of fuel
m_{F_0}	Inlet mass fraction of fuel
m_{ox}	Mass fraction of oxidant
m_p	Mass fraction of combustion product
P	Pressure
$p(f)$	Probability density function,pdf
p_0	Defined in eq. (2.33)
R	Universal gas constant
R_A	Outer radius of annular air jet
R_F	Radius of central fuel jet
s_f	Standard deviation of $\bar{f}$
S_P	The source term associated with the variable at the central nodal point
S_u	The source term that contains all other terms dealing specifically with the variable at the point
S_ϕ	The total volumetric source term for ϕ
T	Temperature
t	Time
u, v	Mean velocity components, axial and radial direction, respectively
u_{air}	Inlet mean velocity of air
u_{fu}	Inlet mean velocity of fuel
u_{max}	Maximum air velocity defined in eq. (3.21)
u_τ	Friction velocity
W	Molecular weight of the mixture

W_A, W_F, W_P	Molecular weight of air, fuel and products, respectively
(x, r)	Axial and radial coordinates, respectively
y^+	Reynolds number based on a velocity scale of the turbulence
α	Constant of two delta functions pdf
β	Constant in eq. (3.28)
Γ	Diffusion coefficient
Γ_ϕ	Diffusion coefficient for ϕ
δ	Thickness of the boundary layer
ϵ	k-dissipation rate
η	Power law constant defined in eq. (3.20)
κ	Experimental constant
λ	Constant in eq. (3.23)
λ_a	Constant in eq. (3.25)
μ	Dynamic viscosity coefficient
$\tilde{\mu}$	The value of f with maximum probability of occurrence
μ_E	Effective viscosity
μ_L	Laminar viscosity
μ_t	Turbulent viscosity
ξ	Defined in eq. (2.9)
ρ	Density
$\bar{\rho}$	Mean value of ρ
$\tilde{\sigma}$	Variance
σ	Constant of turbulence model

τ	Shear stress
ϕ	Scalar variable
$\bar{\phi}$	Mean value of ϕ

Subscripts

A_0	fuel input stream
F_0	air input stream
j	N, S, E, W cell faces

CHAPTER I

INTRODUCTION

1.1. Background

Generally, in a turbulent, non-premixed reacting flow, the fuel and oxygen concentration fluctuations have measurable statistical values which vary from one location to another in the flame zone. Figure 1 is a sketch of a recirculating combustor flow for both laminar and turbulent diffusion flame. The central stream is the fuel flow and the annular stream is the oxidizer flow, often air. According to the theory of laminar diffusion flames [1,2] [1], upon assuming that the rate of chemical reaction between fuel and oxidant is infinite, the combustion process can be divided into two regions. In region I, only fuel and products of combustion exist, and in region II, only oxidant and products exist. Combustion only occurs along a line of perfect stoichiometry (Fig. 1). But for turbulent combustion, because of the effects of the turbulence (or intermittence), there is the possibility of fuel existing in the region II; and also, the possibility for oxidant existing in region I (Fig. 1). Even if the assumption is kept that the rate of chemical reaction is infinite, because of the concentration fluctuations, it is possible that the fuel and oxidant may exist at the same spatial locations but different times, and then the chemical reaction may occur over a large region or area in the chamber, not just along a stoichiometry line. This effect has been observed experimentally by Bilger et al. [3], and by El Ghobashi [4]. Consequently, it is appropriate to treat the fuel and oxidant mass fractions as random variables, and use a statistical treatment of the reaction processes by means of probability density functions (pdf) when

[1] 1 Refers to the reference numbers given in REFERENCES.

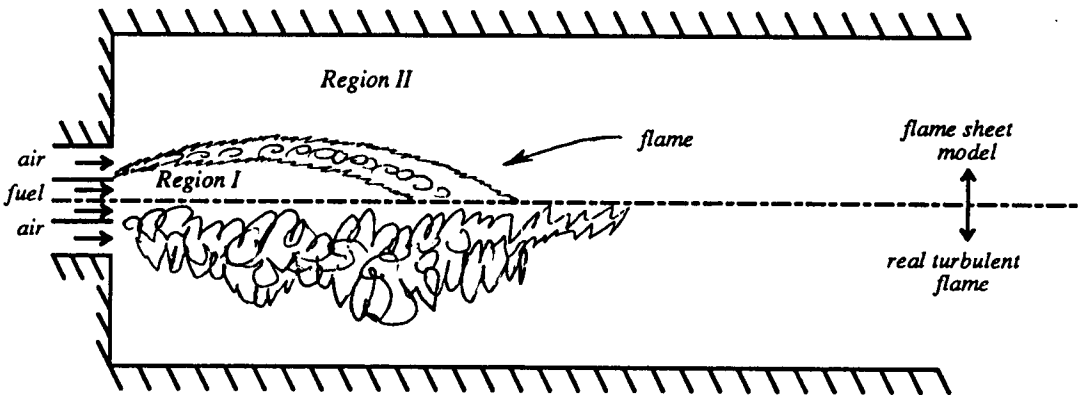

Figure 1. Schematic of "Over-Ventilated" Diffusion Flame in Combustor

attempting to compute turbulent combustion flows.

Probability density functions have been used in the study of turbulent reactive flows for at least 35 years. The literature on the different aspects of pdf theory and application become extensive during the 1970's [5,6]. In the application of pdf theory, two computational approaches to the determination of the pdf's were taken. In one approach parametric pdf functions are assumed and then evaluated or defined at each point of the computed combustor flow by fitting the function to the computed local mean value and variance of a flow variable such as a conserved scalar transported property. But, an important question of computational modeling of combustor flows is the question of whether the pdf approach is necessary to account for turbulent fluctuations on the predicted "mean" flow field quantities, which should be the time (or ensemble) averaged flow field quantities. Recently, Khalil [6] provided an excellent review of the model hierarchy for predicting confined turbulent diffusion flames which included the use of pdf's. In this reference, the need for the pdf applications was to improve the agreement

between predicted results and experimental data, obtained in a variety of combustors, including temperature, species, and velocity fields. However, it was not clear from the referenced literature that all the initial and boundary conditions for the computed flows and the experimental flows were equal; nor was it clear how closely the boundary conditions used in the calculations matched the experiments. Therefore, the present work was undertaken to investigate the use of the parametric pdf method to compute non-premixed diffusion flames in cylindrical combustors with the focus on how "sensitive" the computed solutions were to input and boundary condition modeling.

1.2. Objective of Present Study

The purpose of this work was to study the sensitivity of calculated turbulent diffusion flames in cylindrical combustors. The sensitivity study reported here was done to answer the following questions: (1) How sensitive is the predicted flame and flow field structure to the inlet mean velocity and turbulence level of the fuel and air streams?; (2) Is the sensitivity greater or less, with or without, the pdf approach ?; (3) Do the predicted flow field variables differ significantly from one another such that the cost of using a pdf approach is justified. (Numerical solutions based on using pdfs take longer to compute and are thus more expensive.) The study was done with and without the use of probability density functions (pdf's) to relate the local average density and temperature of the computed flow, to a local average species concentration and its variation. To perform the computations with pdf's, two-parameter pdf functions were used that were previously reported in the literature [5,7,]. They were reviewed by Khalil [6].

To carry out this study, a finite-difference model of a cylindrical combustor was constructed based on a version of the Spalding-Patankar SIMPLE (Semi-

Implicit Method for Pressure Linked Equations) algorithm [8]. The assumed combustor had a central inlet fuel stream and an annular inlet air stream, Fig. 2. For all cases computed, the same finite difference mesh, turbulence transport model and boundary and inlet conditions were applied. The differences that resulted in the predicted solutions are due to the using, or not using a pdf model, and, to the different values of input fuel and air mean velocity and turbulence levels established for the comparison cases. For the computed and compared cases, the fuel and oxidizer input velocity ratio was held constant, which kept the fuel/air ratio (or overall flame stoichiometry) constant for all calculations.

In CHAPTER III, the governing conservation equations of turbulent reacting flow are presented. All cases computed are listed in CHAPTER IV. Also, in CHAPTER IV, comparisons of the calculated results are discussed. Finally, in CHAPTER V, the Summary and Conclusions of the work are presented.

In the next chapter, there is a brief review of pdf models for turbulent non-premixed flames (or turbulent diffusion flames).

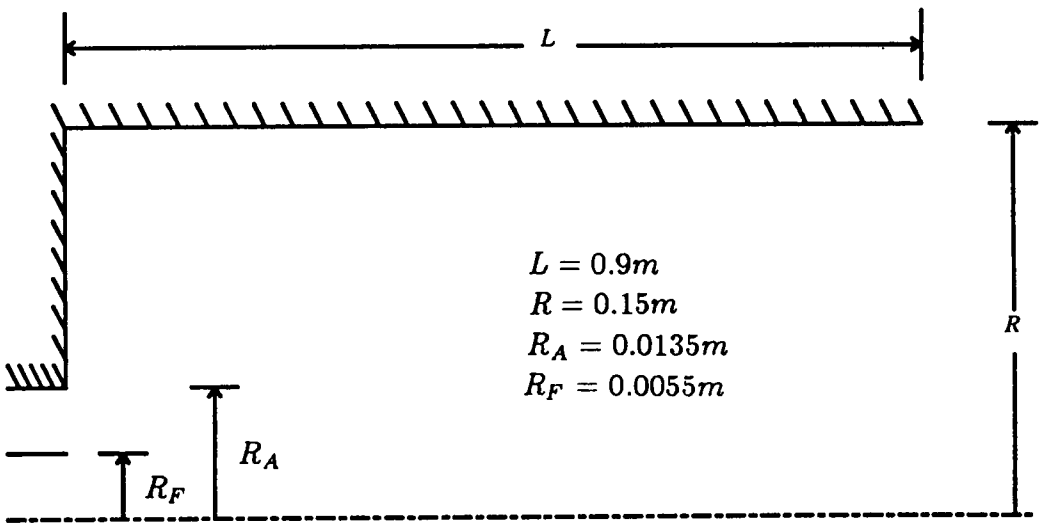

Figure 2. Schematic and Dimensions of Modeled Combustor

CHAPTER II

PDF MODELS FOR TURBULENT DIFFUSION FLAMES

2.1. Determination and Use of PDF'S

In the application of pdf theory, there are two ways to determine the probability density functions that have been predominantly used in the past [9]. One way is that parametric pdf functions are assumed and then evaluated or defined at each point of the computed combustor flow by fitting the function to the computed local mean value and variance of a flow variable such as a conserved scalar transported property [1,6]. For example, at each point in the flow, a convection-diffusion scalar transport equation for a species concentration, $\bar{f}$, (mass fraction or normalized mass fraction) and an equation modeled to predict the distribution of the variance of the mass fraction, g, can be solved. Then an assumed function for the pdf, $p(f)$, can be fully determined in terms of its two parameters $(\bar{f}, g)$ by being fit to the values of $\bar{f}$ and g at each flow field point by requiring that

$$\bar{f} = \int_f f p(f) df \tag{2.1}$$

and

$$g = \overline{(f - \bar{f})^2} = \overline{f^2} - \bar{f}^2 = \int_f (f - \bar{f})^2 p(f) df \tag{2.2}$$

The function $p(f)$ must also satisfy the requirement that

$$\int_f p(f) df = 1 \tag{2.3}$$

Note that one standard deviation for $\bar{f}$ is

$$s_f = \sqrt{g} \tag{2.4}$$

In practical terms, in order to perform the "fit", an elaborate table (or set of tables) is constructed, and then used during the computation to obtain $p(f)$ at each point where $\bar{f}$ and g are computed as flow field variables [7].

In this study, this approach to pdf determination was applied to the computation of recirculating flow in a cylindrical combustor, in a standard geometry: co-axial, two-stream, fuel-oxidizer inlet flow to a sudden-expansion combustor geometry, Fig. 2.

The alternate approach to the determination of $p(f)$ at a each computational point is to create or model an equation, or set of equations that yields the creation and transport of the pdf from point to point in terms of the first and higher order correlations of the fundamental Navier-Stokes, or Reynolds-averaged transport equations [9,10,11]. Thus, the point-by-point functional behavior of the pdf is determined in the course of the flow field solution by solving non-linear evolution equations for the pdf.

In either case, the outcome is the pdf distributions in the flow field. Then, given the pdf at each point, the mean values of selected thermodynamic variables can be obtained in terms of the probabilistic distributions provided by the pdf. For example, if ϕ is a variable that depends on the concentration, f, then the mean value of ϕ at a point in the flow can be obtained as

$$\bar{\phi} = \int_f \phi(f) p(f) df \tag{2.5}$$

The next section will give the relationship between scalar variables with a mixture mass fraction related variable, f.

2.2. Thermal Equation of State

2.2.1. Combustion Chemistry

The combustion chemistry selected was that of the methane $(CH_4) - air$ system. The simple one-step chemical reaction model was used:

on a mole basis

$$CH_4 + 2O_2 + 7.25N_2 \longrightarrow CO_2 + 2H_2O + 7.25N_2 \tag{2.6}$$

on a mass bass

$$1^{\#}CH_4 + 4^{\#}O_2 + 13.16^{\#}N_2 \longrightarrow 2.75^{\#}CO_2 + 2.25^{\#}H_2O + 13.16^{\#}N_2 \tag{2.7}$$

The fuel to air mass ratio, i, is

$$i = \frac{1}{17.16} = .0583$$

The combustion process was modeled as an unpremixed diffusion flame using a flame-sheet approach which was based on the infinitely fast chemical reaction assumption. Many chemical reactions have high rates and can be considered complete as soon as the reactants are mixed. If the Damkohler number N_D is very small, where N_D was defined as the ratio of a characteristic reaction time to a mixing time, by Damkohler [12], the turbulent flame can be approximated adequately with the fast-chemistry assumption. According to Bilger [13], this assumption implies that the instantaneous molecular-species concentrations and the temperature are functions only of the conserved scalar concentration at that instant. With this assumption, a conserved scalar, which is a linear combination of unpremixed reactants, fuel and oxidant, is obtained point by point in a flow by solving a transport

equation. Since the species concentrations are directly related to the conserved scalar, the thermodynamic state variables are also obtained directly in terms of the scalar, f. Therefore, the need to evaluate mean reaction rates is removed. The scalar flame sheet model was originally used for laminar flames in tubes [14], and boundary layers [15], and in turbulent flows in a variety of combustor geometries [6]. It has the merit of simplicity and computational economy which is valuable when computing flows with recirculation.

2.2.2. Flame Sheet Model

In the present study a transport equation was solved for a variable, $\bar{f}$, that is related to the mean fuel fraction variable. The variable $\bar{f}$ is called herein the mixture mass fraction, and is defined as the mean value of a scalar variable f. f is defined as

$$f = \frac{\xi - \xi_{A_0}}{\xi_{F_0} - \xi_{A_0}} \tag{2.8}$$

where

$$\xi = m_F - i m_A \tag{2.9}$$

where m_F is the fuel mass fraction and m_A is the air mass fraction. The parameter i is the stoichiometric fuel/air ratio. The subscript F_0 refers to the fuel input stream and A_0 refers to the air input stream. As defined, f varies from 1.0 in the fuel stream to 0.0 in the air stream. Thus, for all points where ξ=0, or f=f_{stoich}=-$\xi_{A_0}/(\xi_{F_0}$-$\xi_{A_0})$, a stoichiometric flame sheet has been located in the flow field. For the methane-air system, for which i=0.0583, this corresponds to the locus of points where $f = f_{stoich} = 0.055$. As discussed earlier, in the flame

sheet model applied without pdf's, only fuel and products of combustion exist on the fuel jet side of the flame, and on the air-side, only air and products of combustion exist on the air side of the flame. The mean value of f is just $\bar{f}$. The variable $\bar{f}$ is a conserved scalar with no source term when the following two assumptions are made:

(a) That the turbulent transport coefficients for the reactants and the products are equal.

(b) That fuel and air combine or react only and always in a stoichiometric ratio.

Because of the simple one-step chemical reaction assumption and fast chemical reaction assumption, the fuel mass fraction, m_F, the air mass fraction, m_A, and the product mass fraction, m_P, can be determined by just solving a transport equation of mixture mass fraction, f. The reason is:

If $f < f_{stoich}$, then

$$m_F = 0 \tag{2.10}$$

and

$$m_A = m_{A_0}\left[1 - \frac{f}{f_{stoich}}\right] \tag{2.11}$$

If $f > f_{stoich}$, then

$$m_A = 0 \tag{2.12}$$

and

$$m_F = m_{F_0}\left[\frac{f - f_{stoich}}{1 - f_{stoich}}\right] \tag{2.13}$$

For both cases, the combustion product m_P is

$$m_P = 1. - m_F - m_A \tag{2.14}$$

2.2.3. Temperature, Density and Molecular Weight Functions

Usually, the temperature, T, is not just a function of the mixture mass fraction f. It is a function of f and enthalpy h. Since the total enthalpy is a conserved scalar variable like mixture mass fraction, f, and the flow is adiabatic flow, in the present work, enthalpy, h, is a function only of f

$$h(f) = h_{A_0} + f \cdot (h_{F_0} - h_{A_0}) \tag{2.15}$$

So

$$T(f,h) = T(f,h(f)) = T(f) \tag{2.16}$$

Specifically,

$$T(f) = (h(f) - m_F H_F)/c_p(f) \tag{2.17}$$

where $c_p(f)$ is the specific heat of the mixture, and H_F is the heat of combustion of fuel. The specific heat, $c_p(f)$, is the mass-weighted specific heat of the mixture, defined in terms of constant specific heats assumed for the species in the mixture. The linear relationship between f and other scalar properties is shown in Figure 3.

The molecular weight of the mixture is $W(f)$, given by

$$W(f) = \frac{1}{\frac{m_A(f)}{W_A} + \frac{m_F(f)}{W_F} + \frac{m_P(f)}{W_P}} \tag{2.18}$$

In this equation W_A, W_F, and W_P are the molecular weight of air, methane and products of combustion, respectively.

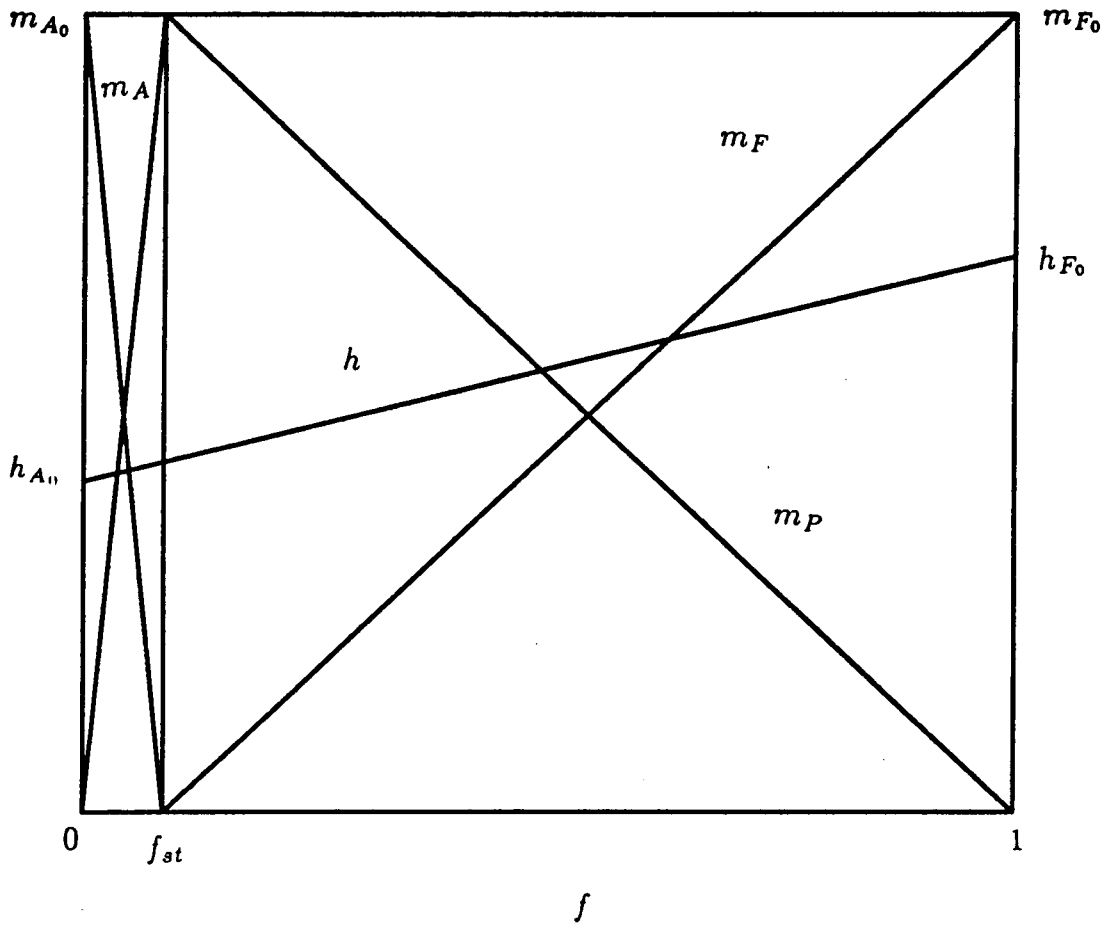

Figure 3. Relation between f and Scalar Properties

Density is determined from the equation of state

$$\rho(f) = \frac{PW(f)}{RT(f)} \tag{2.19}$$

where R is the universal gas constant.

The simple linear formulations for the temperature and density functions given by equations (2.15), (2.16) and (2.17) were used in the present study with constants appropriate to the methane-air system.

When a flow field solution is obtained without a pdf application, then the mean temperature and density are specified at each point of the mesh from equations (2.15), (2.16) and (2.17) with $\bar{f}$ replacing f. However, when a pdf is used to obtain the mean values of ρ and T, then they are obtained from

$$\overline{T} = \int_0^1 T(f)p(f)df \tag{2.20}$$

$$\bar{\rho} = \int_0^1 \frac{PW(f)}{RT(f)} p(f)df \tag{2.21}$$

2.3. PDF Models

The study used two types of pdf's, both previously reported in the literature [6]. They are given below.

"Model 2 PDF" [6]

In this model, the probability density function is represented by two delta functions. This simplest form of pdf was previously used by Spalding [5], El Ghobashi [16], Khalil et al. [17], Richter [18], and Gosman [19]. The two-delta function pdf is determined by $\bar{f}$ and g in the following way. Define

$$f_+ = \bar{f} + \sqrt{g} \tag{2.22}$$

and

$$f_- = \bar{f} - \sqrt{g} \tag{2.23}$$

then

$$p(f) = \alpha * \delta(f - f_-) + (1 - \alpha) * \delta(f - f_+) \tag{2.24}$$

where $\alpha = 0.5$.

When $f_+ > 1.$, let $f_+ = 1$ and

$$\alpha = \frac{1 - \bar{f}}{1 - \bar{f} + \sqrt{g}} \tag{2.25}$$

and then

$$p(f) = \alpha * \delta(f - f_-) + (1 - \alpha) * \delta(f - 1) \tag{2.26}$$

When $f_- < 0$, let $f_- = 0$ and

$$\alpha = \frac{\sqrt{g}}{\bar{f} + \sqrt{g}} \tag{2.27}$$

and then

$$p(f) = \alpha * \delta(f) + (1 - \alpha) * \delta(f - f_+) \tag{2.28}$$

$\delta(\ )$ is the Dirac delta function.

This two delta function pdf was shown by Jones [20] to be unsatisfactory in comparison with Kent and Bilger's measurement [21] on turbulent diffusion flame.

"Model 3 PDF" [6]

This model was first suggested by Naguib [5] and El Ghobashi [4] and has been widely used in calculation of furnace and combustor chamber flow [6,22,23, et al]. For this model, the probability density function is a Clipped-Gaussian function. Reference [6] provides additional details of this function. The probability density

is given by

$$p(f) = \frac{1}{\sqrt{2\pi}\tilde{\sigma}} \exp\left(-\frac{1}{2}(\frac{f-\tilde{\mu}}{\tilde{\sigma}})^2 \right)[D(f) - D(f-1)]$$

$$+A\delta(f) + B\delta(f-1) \tag{2.29}$$

where $\tilde{\mu}$ is the value of f giving maximum probability; $\tilde{\sigma}$ is the variance; $D(f)$ is the Heaviside step function defined as, $\mathrm{D}(\xi) = 0$, $\xi < 0$ and $\mathrm{D}(\xi) = 1$, $\xi > 0$.

Reference 6 gives

$$\bar{f} = B + \int_0^1 \frac{f}{\sqrt{2\pi}\tilde{\sigma}} \exp(-\frac{1}{2}(\frac{f-\tilde{\mu}}{\tilde{\sigma}})^2)df \tag{2.30}$$

and

$$g = B + \int_0^1 \frac{f^2}{\sqrt{2\pi}\tilde{\sigma}} \exp(-\frac{1}{2}(\frac{f-\tilde{\mu}}{\tilde{\sigma}})^2)df - \bar{f}^2 \tag{2.31}$$

where

$$B = \int_1^\infty p_0(f)df \tag{2.32}$$

$$A = \int_{-\infty}^0 p_0(f)df$$

for

$$p_0(f) = \frac{1}{\sqrt{2\pi}\tilde{\sigma}} \exp(-\frac{1}{2}(\frac{f-\tilde{\mu}}{\tilde{\sigma}})^2) \tag{2.33}$$

The values of $\tilde{\mu}$ and $\tilde{\sigma}$ are determined from a table, provided by Ref. [24], in terms of $\bar{f}$ and g, by searching. The average value of any property ϕ that depends on f can be obtained from:

$$\bar{\phi} = A\bar{\phi}_0 + B\bar{\phi}_1 + \int_0^1 \frac{\phi(f)}{\sqrt{2\pi}\tilde{\sigma}} \exp(-\frac{1}{2}(\frac{f-\tilde{\mu}}{\tilde{\sigma}})^2)df \tag{2.34}$$

where $\bar{\phi}_0$ and $\bar{\phi}_1$ are the values of ϕ at $f = 0$ and $f = 1$, respectively.

2.4. Density Dependent Solution Behavior

Finally, one thing should be mentioned. An important requirement for the application of the pdf theory is this: in order for the application of the pdf to result in any difference in computed flows, the density should vary significantly as f varies over its range. To give an illustration, if in a combustion process the density, ρ, is essentially constant or independent of the local stoichiometry of the flame, and thus is more or less independent of the local fuel concentration, f, then the application of a pdf to the computation of the flow may not yield any appreciable difference in the structure of the flow except for temperature distributions. The density ρ obtained from a probabilistic approach such as

$$\bar{\rho} = \int_f \rho(f) p(f) df \tag{2.35}$$

will be the same as $\bar{\rho}$ obtained from

$$\bar{\rho} = \bar{\rho}(\bar{f}) = \frac{PW(\bar{f})}{RT(\bar{f})} \tag{2.36}$$

For such a fuel-oxidant combination, the predicted mixing and recirculation or flow structure should be the same with and without a pdf approach since f would not affect ρ, nor, then, the turbulent viscosity, μ_t. So, when selecting combustor conditions for the investigation of sensitivity of predicted results to pdf applications, it is important to select a fuel-oxidant combination that produces a significant density variation in the flame and combustion zones and exhibits a sensitivity to variations in f over some range of stoichiometry. This sensitivity can be determined from the thermal equation of state by simply plotting ρ versus f as f varies from zero (no fuel) to 1.0 (all fuel), for pressures in the range expected in the combustor. Figure 4 shows such plots for the hydrogen-air and the methane-air

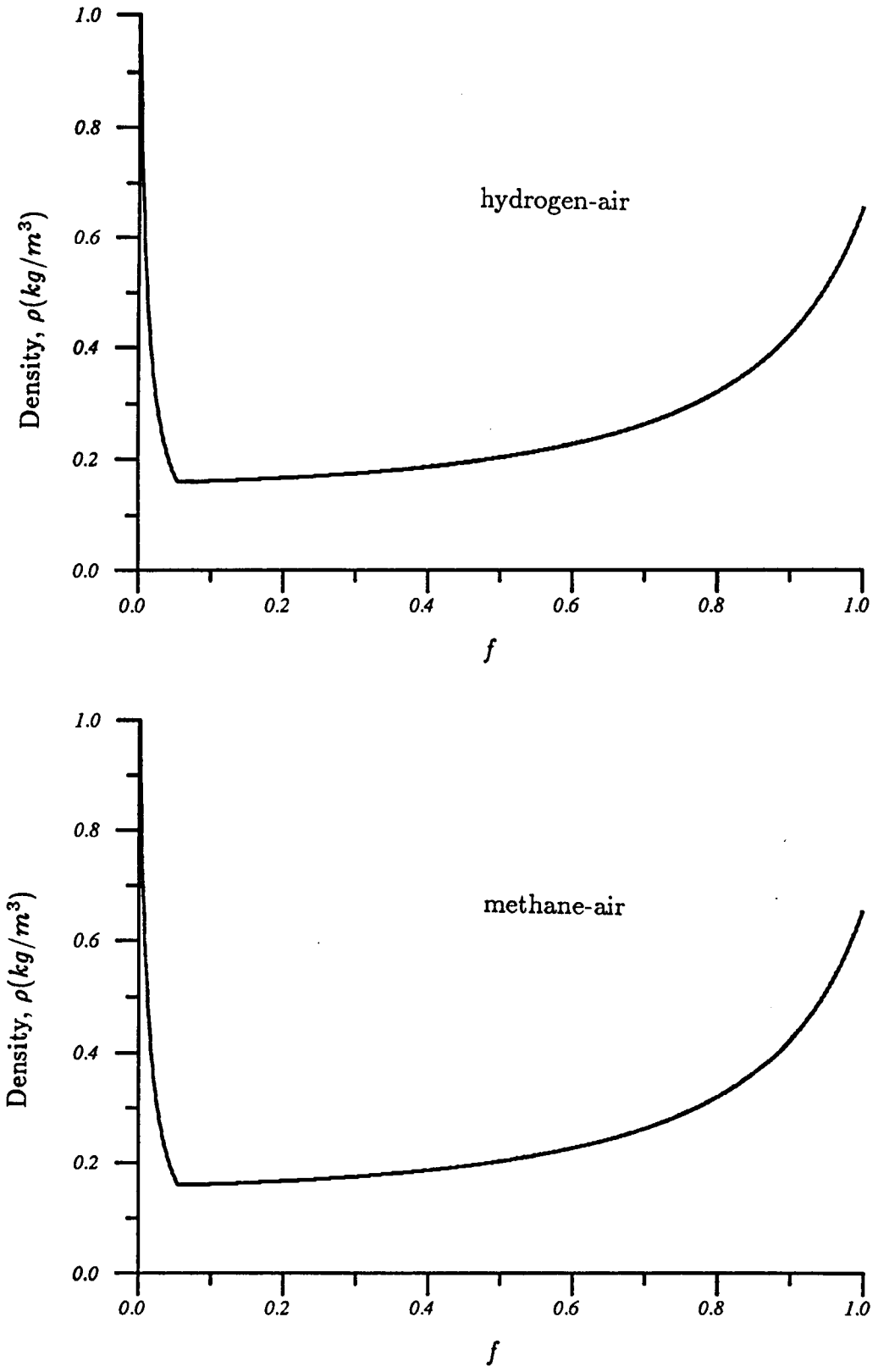

Figure 4. Variation of Density with f

systems. The $\rho - f$ sensitivity is greatest on the fuel-lean side for both H_2-air and methane-air, Fig. 4. This $\rho - f$ coupling could affect the numerical solution significantly, say, through the effect of ρ on the local turbulent viscosity; if, for example, a significant fluctuation in f about its fuel-lean values was occurring near a wall stagnation (reattachment) point, then one might expect the predicted flow field structure to be sensitive to the application of a pdf approach through its effect on ρ and μ_t, and hence flow reattachment, at the wall stagnation point.

Note that the geometry of a combustor can influence the predicted f distributions, and thus may or may not result in "sensitive"solutions. So, the sensitivity study can be affected by the assumed combustor geometry. In the present study, the geometry was fixed.

CHAPTER III

PREDICTION TECHNIQUES

3.1. Governing Equations

In the present study, the flow field distributions of the mean velocity components, u and v, turbulence kinetic energy, k, k-dissipation rate, ϵ, mean fuel fraction variable, $\bar{f}$, and its variance, g, were all computed by numerically solving a conservation-transport type equation of the form

$$\frac{1}{r}\left\{\frac{\partial}{\partial x}(\rho u r\phi)+\frac{\partial}{\partial r}(\rho v r\phi)-\frac{\partial}{\partial x}\left(r\Gamma_\phi\frac{\partial\phi}{\partial x}\right)-\frac{\partial}{\partial r}\left(r\Gamma_\phi\frac{\partial\phi}{\partial r}\right)\right\}=S_\phi \qquad (3.1)$$

where ϕ is a scalar variable, u and v the mean velocity components in the axial and radial direction, respectively, Γ_ϕ a diffusion coefficient for ϕ, and S_ϕ is the volumetric source term for ϕ. For $\phi = 1$, equation (3.1) is a total mass continuity equation. A variety of references discuss this flow model [25,26]. Table 1 shows the variables, ϕ, solved for in this study, their coefficients, and source terms. Table 2 gives the values of the various constants of the model.

The turbulence model used in this study is the two-equations $k-\epsilon$ model [27,28]. The effective viscosity was given by

$$\mu_E = \mu_t + \mu_L \qquad (3.2)$$

where

$$\mu_t = 0.09\bar{\rho}\frac{k^2}{\epsilon} \qquad (3.3)$$

and

$$\mu_L = 0.000011$$

μ_t is the turbulent viscosity and $\mu_L$is the laminar viscosity. The general diffusion coefficients are defined as

$$\Gamma_\phi = \mu_E/\sigma_\phi \tag{3.4}$$

for fully turbulent flow.

TABLE 1

Source Terms and Exchange Coefficients Used

in the General Equation of ϕ

ϕ	Γ_ϕ	S_ϕ
1		0
u	μ_E	$-\frac{\partial p}{\partial x} + S^u$
v	μ_E	$-\frac{\partial p}{\partial r} - 2\mu_E v/r^2 + S^v$
k	μ_E/σ_k	$G - C_D\bar{\rho}\epsilon$
ϵ	μ_E/σ_ϵ	$(C_1\epsilon G - C_2\bar{\rho}\epsilon^2)/k$
$\bar{f}$	μ_E/σ_f	0
$\bar{h}$	μ_E/σ_h	0
g	μ_E/σ_g	$C_{g_1}\mu_E(\nabla\bar{f})^2 - C_{g_2}\bar{\rho}\frac{\epsilon}{k}g$

In TABLE 1 certain quantities are defined as following:

$$S^u = \frac{\partial}{\partial x}\left(\mu\frac{\partial u}{\partial x}\right) + \frac{1}{r}\frac{\partial}{\partial r}\left(r\mu\frac{\partial v}{\partial x}\right) \tag{3.5}$$

$$S^v = \frac{\partial}{\partial x}\left(\mu\frac{\partial u}{\partial r}\right) + \frac{1}{r}\frac{\partial}{\partial r}\left(r\mu\frac{\partial v}{\partial r}\right) \tag{3.6}$$

$$G = \mu_E\left[2\left\{\left(\frac{\partial u}{\partial x}\right)^2 + \left(\frac{\partial v}{\partial r}\right)^2 + \left(\frac{v}{r}\right)^2\right\} + \left(\frac{\partial u}{\partial r} + \frac{\partial v}{\partial x}\right)^2\right] \tag{3.7}$$

$$\nabla\bar{f} = \frac{\partial\bar{f}}{\partial x}\hat{i}_x + \frac{\partial\bar{f}}{\partial r}\hat{i}_r \tag{3.8}$$

TABLE 2

Combustion Model Constants

Constant	Value
σ_k	1.0
σ_ϵ	1.22
σ_f	0.9
σ_h	0.9
σ_g	0.9
C_1	1.44
C_2	1.92
C_{g1}	2.8
C_{g2}	2.0

3.2. Boundary Conditions

3.2.1. Fuel Fraction and its Variance

Boundary conditions for all ϕ must be prescribed: in particular, for the inlet streams, one usually prescribes the mean axial, radial, and swirl velocities u, v, w, if any, the turbulence kinetic energy, k, the rate of dissipation of turbulence kinetic energy, ϵ, and the effective viscosity, μ_E distributions across the fuel and air streams. At walls, for high Reynolds number turbulent flow, law-of-the-wall "wall functions "were used to yield a slip-velocity that matches a law-of-the-wall boundary layer profile. Consistent functions were used that provide k and ϵ at the wall by iterative procedures that develop the wall values of k and ϵ during the course of the solution procedure. The boundary conditions for $\bar{f}$ and g were:

over the fuel stream

$$\bar{f}_{F_0} = 1.0 \tag{3.9}$$

$$g_{F_0} = 0.0 \tag{3.10}$$

over the air stream

$$\bar{f}_{A_0} = 0.0 \tag{3.11}$$

$$g_{A_0} = 0.0 \tag{3.12}$$

on the centerline and on the top wall

$$\frac{\partial \bar{f}}{\partial r} = 0 \tag{3.13}$$

$$\frac{\partial g}{\partial r} = 0 \tag{3.14}$$

on the vertical wall and across the outlet of the combustor

$$\frac{\partial \bar{f}}{\partial x} = 0 \tag{3.15}$$

$$\frac{\partial g}{\partial x} = 0 \tag{3.16}$$

Since an adiabatic boundary condition was assumed, the boundary conditions for $\bar{h}$ were:

on the centerline and on the top wall

$$\frac{\partial \bar{h}}{\partial r} = 0 \tag{3.17}$$

on the vertical wall and across the outlet of the combustor

$$\frac{\partial \bar{h}}{\partial x} = 0 \tag{3.18}$$

3.2.2. Inlet Conditions for u, v, k, ϵ, and μ_E

The inlet conditons for u, v, k, ϵ, and μ_E were varied during the study to determined the effects of the different profiles shapes and their magnitudes on the structure of the predicted flows.

Axial and Radial Velocity

The first calculations were carried out using a uniform (flat) axial velocity profile for the fuel stream and a double power-law distribution for the axial velocity of the annular air stream. For both streams, the v-velocity was set to zero. These conditions are shown below:

Fuel Stream (Central, axisymmetric)

$$u = U_{F_0} \qquad r \leq R_F \tag{3.19}$$

Air Stream (Annular, axisymmetric)

$$u = \begin{cases} u_{max}\left(\frac{r-R_F}{\delta}\right)^{\frac{1}{\eta}} & \text{if} \quad R_F < r < R_F + \delta \\ u_{max} & \text{if} \quad R_F + \delta < r \leq R_A - \delta \\ u_{max}\left(\frac{R_A-r}{\delta}\right)^{\frac{1}{\eta}} & \text{if} \quad R_2 - \delta < r \leq R_A \\ 0 & \text{if} \quad r > R_A \end{cases} \tag{3.20}$$

and

$$\delta = 0.22(R_A - R_F).$$

The parameter δ is the assumed thickness of the defect part of the power law velocity profile on the upper and lower surfaces of the annular jet and u_{max} is related to the bulk velocity of the air by the formula

$$u_{max} = \frac{U_{A_0}}{1 - \frac{2\delta}{(1+\eta)(R_2 - R_1)}} \tag{3.21}$$

For both stream, the inlet radial velocity is:

$$v = 0 \tag{3.22}$$

Turbulent Kinetic Energy

for the fuel stream

$$k = \lambda {U_{F_0}}^2 \tag{3.23}$$

for the annular air stream

$$k = l^2 w \frac{\partial u}{\partial r} \tag{3.24}$$

The constant, λ, was varied from $(0.01)^2$ to $(0.05)^2$, to as high as $(0.25)^2$, in order to investigate the effects of the fuel jet turbulence level on the predicted flow field

structure. This corresponded, approximately, to 1%, 5% and 25% fuel stream turbulence levels in the numerical simulation.

Turbulent Dissipation

for the fuel stream

$$\epsilon = \frac{k^{3/2}}{\lambda_a R_F} \tag{3.25}$$

where $\lambda_a = 0.005$.

for the air stream

$$\epsilon = C_\mu k w \tag{3.26}$$

Viscosity

The viscosity for both the fuel and air stream was given by

$$\mu_E = \mu_L + C_\mu \bar{\rho} k^2 / \epsilon \tag{3.27}$$

In the previous equations, w is another form of turbulent dissipation [29] given by

$$w = \frac{u_\tau}{\sqrt{C_\mu}\kappa y} + \frac{6\mu/\rho}{\beta y^2} \tag{3.28}$$

and l is Prandtl's mixing-length. The mixing-length formula used here was suggested by Van Driest,

$$l = \kappa y \left[1 - exp\left(-\frac{y^+}{A^+}\right)\right] \tag{3.29}$$

where

$u_\tau = \sqrt{\tau/\rho}$, evaluated at the wall

$y^+ = u_\tau y/\nu$

$\kappa = 0.41$

$\beta = 0.075$

$A^+ = 26.0$

3.3. Solution Techniques and Finite Difference Formulation

The present solution technique was based on the primitive variable pressure-velocity approach. The basic TEACH code using SIMPLE (Semi-Implicit Method for Pressure-Linked Equation) with a tri-diagonal matrix solver algorithm (TDMA) was used as the starting point in this investigation [8]. The finite difference equations were solved on a two-dimensional grid system with a mesh of 40 by 34 lines, axially and radially, respectively. The finite difference equations for each ϕ are obtained by integrating equation 3.1 over a generalized (finite-volume) control volume and expressing the results in terms of surrounding grid or nodal point values. The convection terms and diffusion terms become surface integrals and the source term, which is linearized and divided into two portions, S_p and S_u, is a volume integral.

$$\int_V S_\phi dV = \int_V {S_P}^\phi (\phi_P + {S_u}^\phi) dV \tag{3.30}$$

${S_P}^\phi$ is the source term associated with the variable at the central nodal point and ${S_u}^\phi$ contains all other source terms that are not linearly dependent on (or are weakly coupled to) the variable ϕ at the point P. To aid in convergence, the ${S_P}^\phi$ term is usually negative while ${S_u}^\phi$ is positive, thus increasing the diagonal dominance of the solution matrix [8]. Table 3 contains the components of the various sources. A hybrid scheme is used for the representation of the convective and diffusive terms over the cell control volume surfaces [8]. The general finite-volume conservation equation is

$$\tilde{a}_P^\phi \phi_P = \sum_j \tilde{a}_j^\phi \phi_j + \tilde{S}_U^\phi \tag{3.31}$$

where

$$\tilde{a}_P^{\phi} = \sum_j \tilde{a}_j^{\phi} - \tilde{S}_P^{\phi} \tag{3.32}$$

The terms with tilde's contain the appropriate areas and volumes associated with the specific finite volume generated by intersecting mesh lines. $\sum_j$ = sum over N, S, E,and W neighbors, thus linking each ϕ-value at a point P with its four neighbors. Equation 3.18 is the form which is solved utilizing the TDMA. The linearized algebraic equations are cast in form containing "residuals." A solution is said to occur by "convergence" of the set of algebraic equations when the maximum of the residuals is reduced to some arbitrary, small numerical value that, in the present study, was about 4×10^{-4}. Details are provided elsewhere [25].

TABLE 3

The Form of the Components of the Linearized Source Term

ϕ	Γ_ϕ	$S_P{}^\phi$	$S_u{}^\phi/V$
1	0	0	0
u	μ_E	0	$-\frac{\partial p}{\partial x} + S^u$
v	μ_E	$-2\frac{\mu_E}{r^2}$	$-\frac{\partial p}{\partial r} + S^v$
k	μ_E/σ_k	$-C_\mu C_D \rho^2 k/\mu_E$	G
ϵ	μ_E/σ_ϵ	$C_2\bar{\rho}\epsilon/k$	$C_1 C_\mu G\rho k/\mu_E$
$\bar{f}$	μ_E/σ_f	0	0
$\bar{h}$	μ_E/σ_h	0	0
g	μ_E/σ_g	$C_{g_1}\mu_E(\nabla\bar{f})^2$	$-C_{g_2}\bar{\rho}\frac{\epsilon}{k}$

CHAPTER IV

RESULTS AND ANALYSIS

4.1. The Cases Evaluated

A basic set of 15 cases was computed. The difference between these cases was due to the absence or use of a pdf, the type of pdf when used, the magnitude of the mean velocity of the input fuel and air streams (Reynolds number effect investigation), and the assigned turbulence level of the fuel stream. In the cases presented here, the turbulence intensity at the center of the annular air stream was held constant at 5%. The cases investigated are shown in TABLE 4 below.

TABLE 4

The Cases Evaluated

Case	Model	U_F m/s	U_A m/s	Turbulent intensity of fuel-stream	Turbulent intensity of air-stream
1	2-δ	7	4.83	1%	5%
2	2-δ	7	4.83	5%	5%
3	C-G	7	4.83	1%	5%
4	C-G	7	4.83	5%	5%
5	2-δ	25	17.2	1%	5%
6	2-δ	86	59.3	1%	5%
7	C-G	25	17.2	1%	5%
8	C-G	86	59.3	1%	5%
9	npdf	7	4.83	1%	5%
10	npdf	7	4.83	5%	5%
11	npdf	25	17.2	1%	5%
12	npdf	86	59.3	1%	5%
13	2-δ	7	4.83	25%	5%
14	C-G	7	4.83	25%	5%
15	npdf	7	4.83	25%	5%

By examining TABLE 4, different cases were chosen for comparison to show the differences in predicted solutions, as they are affected by the type of pdf model and fuel-stream inlet conditions. These cases are as follows.

Cases 1, 2, 5, 6, and 13 correspond to the two-delta function pdf model, and can be compared as follows:

Case 1 vs Case 2 vs 13 - effect of fuel stream turbulence

Case 1 vs Case 5 vs Case 6 - effect of fuel stream mean velocity (or Reynolds number.)

Case 3, 4, 7, 8, and 14 correspond to the Clipped-Gaussian pdf model, and can be compared as follows:

Case 3 vs Case 4 vs 14 - effect of fuel stream turbulence intensity

Case 3 vs Case 7 vs Case 8 - effect of fuel stream mean velocity

Case 9, 10, 11, 12 and 15 represent predictions made without the application of a pdf, and may be compared as follows:

Case 9 vs Case 10 vs 15 - effect of fuel stream turbulence intensity

Case 9 vs Case 11 and 12 - effect of fuel stream mean velocity

Next, the various cases can be compared for the same values of fuel stream turbulence and mean velocity but for the different pdfs used or neglected. Thus, one can compare:

Case 9 vs Case 1 vs Case 3 - effect of no pdf models vs pdf for 1% fuel turbulence and 7 m/s mean velocity

Case 10 vs Case 2 vs Case 4 - effect of no pdf models vs pdf for 5% fuel turbulence and 7 m/s mean velocity

Case 5 vs Case 7 vs Case 11 - effect of pdf model for 1 % fuel turbulence and 25 m/s mean velocity

Case 6 vs Case 8 vs Case 12 - effect of pdf models for 1% fuel turbulence and 86 m/s mean velocity

A summary of the comparisons is provided below.

4.2. Results of the Comparisons

4.2.1. Streamlines Patterns and Recirculation Zones

Fig. 5 shows the differences between three methods (no-pdf, two-delta function pdf, and Clipped-Gaussian pdf) for 7 m/s fuel jet mean velocity and 1% fuel turbulence level. The calculation made with no pdf (case 9) has a shorter recirculation zone than either the two-delta function pdf or the Clipped-Gaussian pdf. The Clipped-Gaussian pdf has the longest recirculation zone. But the differences between these three methods are small.

When increasing the inlet fuel mean velocity from 7 m/s to 25 m/s and 86 m/s, for 1% fuel stream turbulence, the same comparisons between three methods are shown in Figs. 6 and 7. The differences, in the stream line patterns between not using pdf and using a pdf (two-delta function pdf and Clipped-Gaussian pdf), are again very small. Overall, the difference between Fig. 5 with Figs. 6 and 7 are small. The 2-δ and Clipped-Gaussian recirculation zones increase slightly in length as the Reynolds number (mean velocity) of the calculation increase, but for the no pdf calculation, there is essentially no change in length of recirculation zone.

Figures 8 and 9 show the relatively small change in recirculation zone structure that result for each method when increasing the inlet fuel mean velocity (basically the same data of Fig. 5, 6, and 7 are replotted for clarity). For the no pdf cases, no significant changes in recirculation zone structure were observed by increasing the

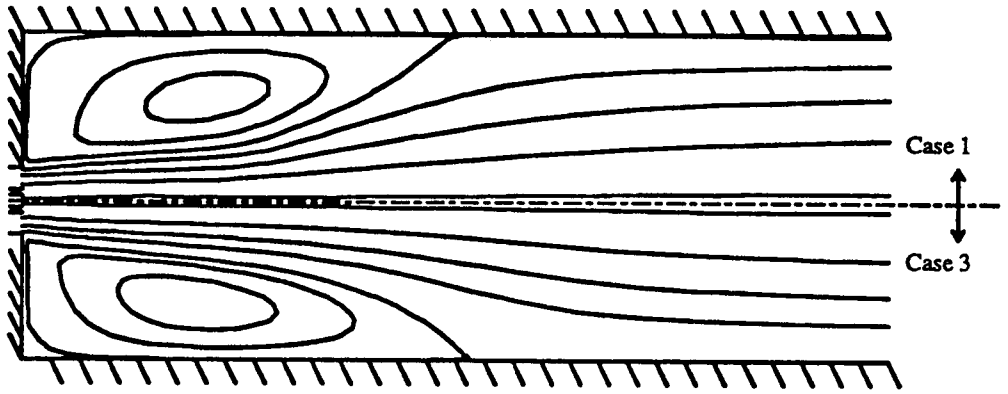

(a) 2-δ functions pdf versus Clipped Gaussian pdf

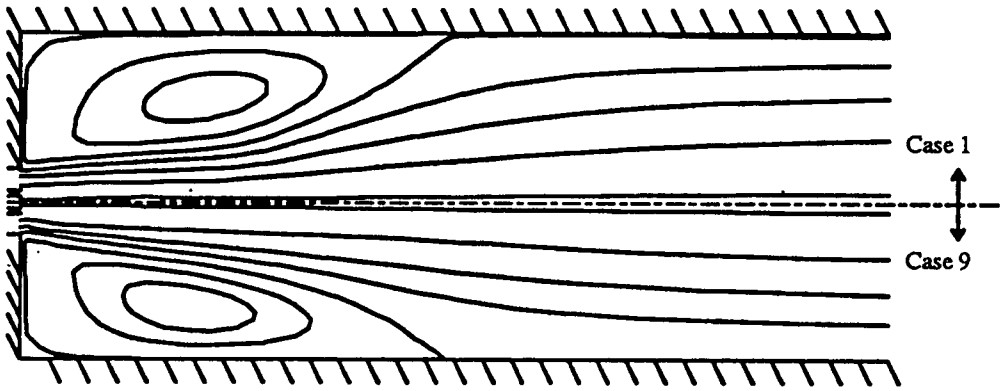

(b) 2-δ functions pdf versus No pdf

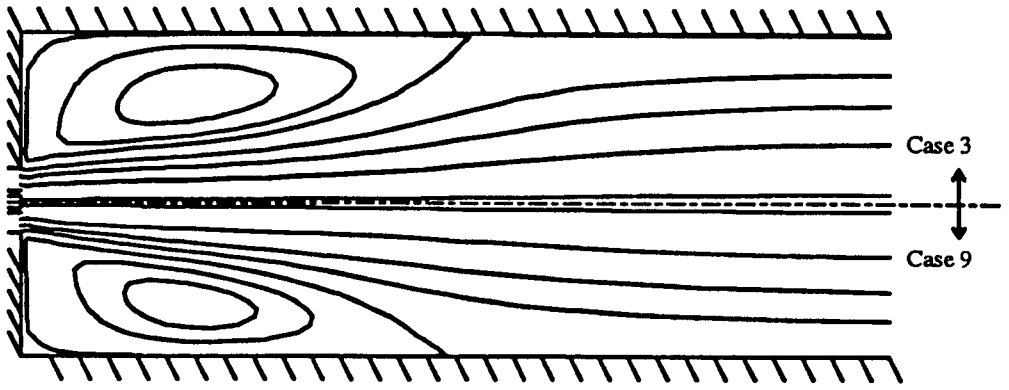

(c) Clipped Gaussian pdf versus No pdf

Figure 5. Comparison of Recirculation Zone Structure Obtained with No-pdf, 2-δ functions PDF, and Clipped-Gaussian PDF for 7 M/S Fuel Mean Velocity, 1% Inlet Fuel Stream Turbulence

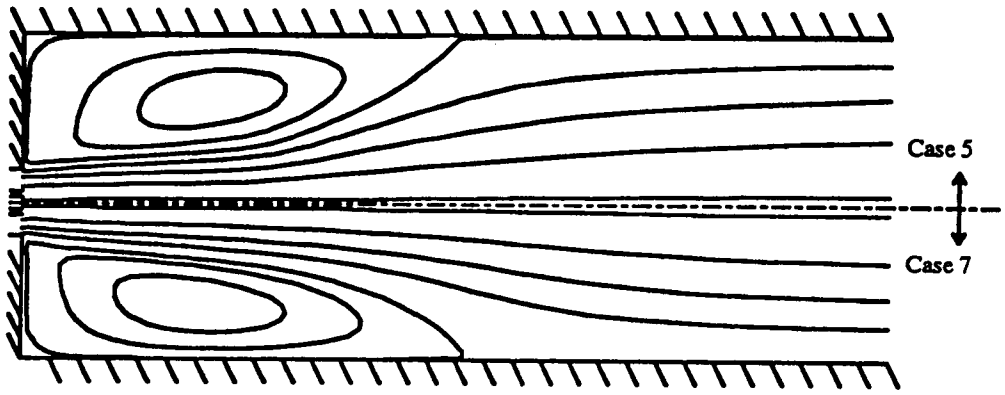

(a) 2-δ functions pdf versus Clipped Gaussian pdf

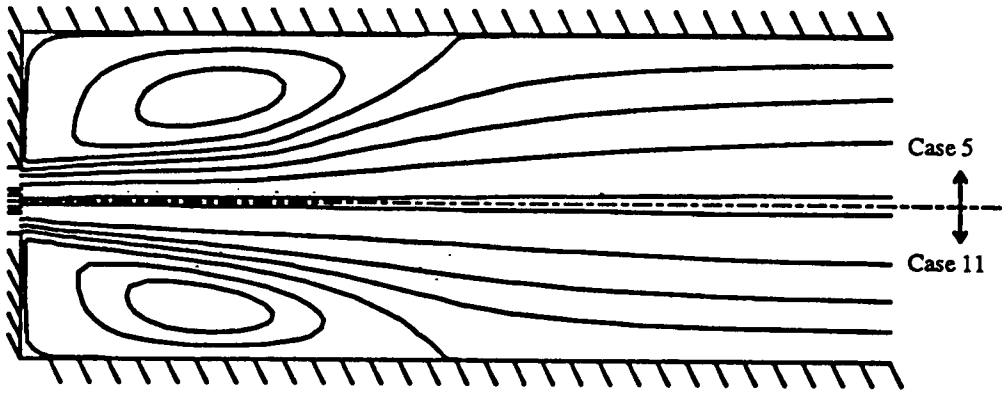

(b) 2-δ functions pdf versus No pdf

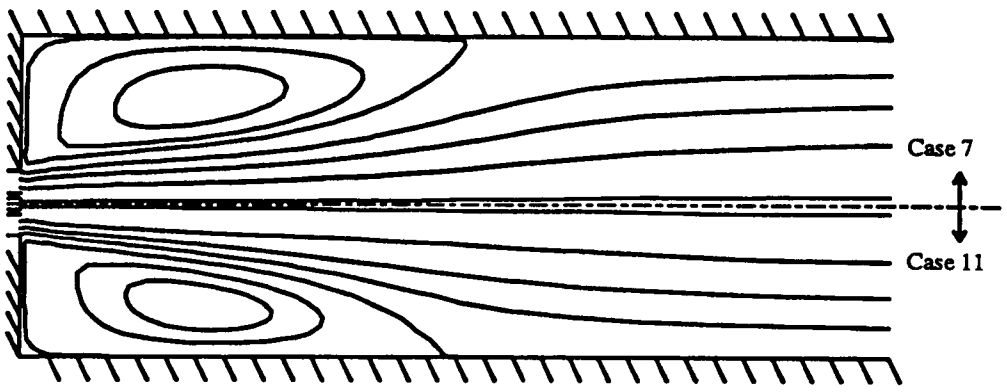

(c) Clipped Gaussian pdf versus No pdf

Figure 6. Comparison of Recirculation Zone Structure Obtained with No-pdf, 2-δ functions PDF, and Clipped-Gaussian PDF for 25 M/S Fuel Mean Velocity, 1% Inlet Fuel Stream Turbulence

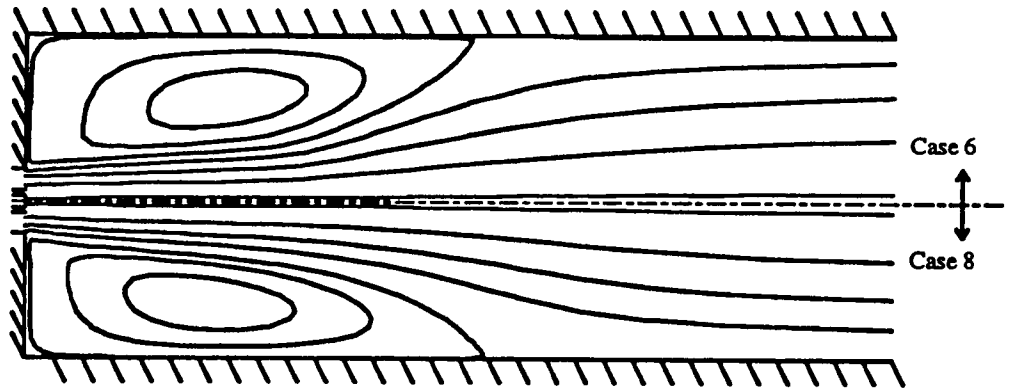

(a) 2-δ functions pdf versus Clipped Gaussian pdf

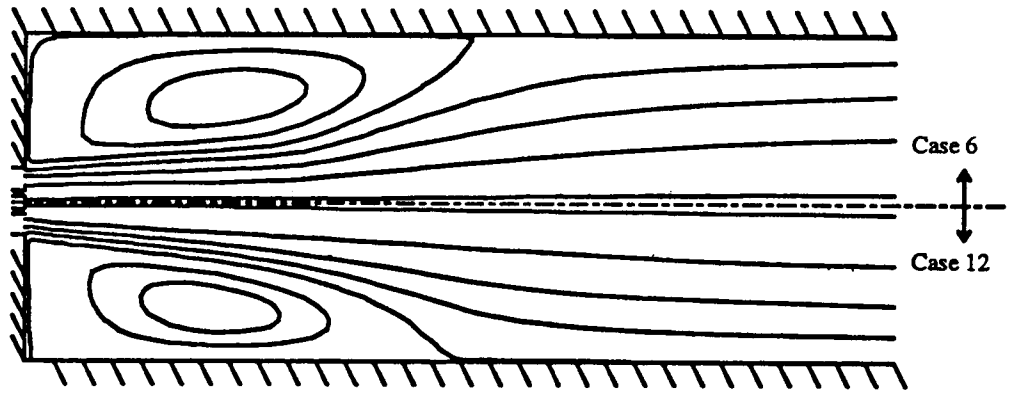

(b) 2-δ functions pdf versus No pdf

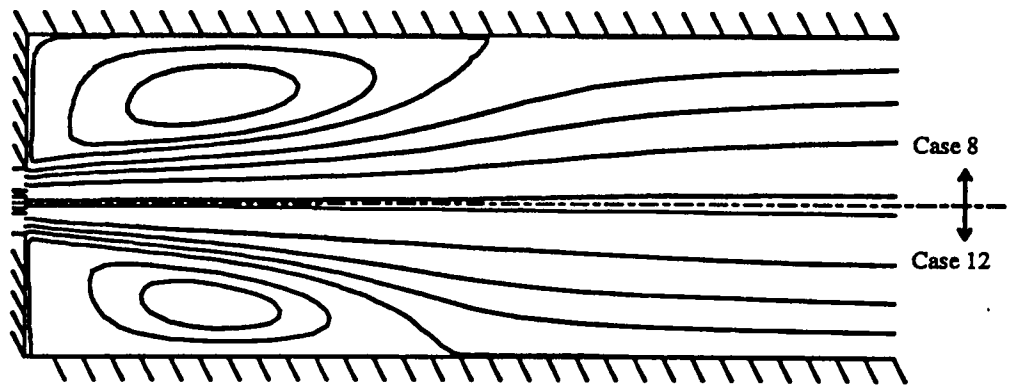

(c) Clipped Gaussian pdf versus No pdf

Figure 7. Comparison of Recirculation Zone Structure Obtained with No-pdf, 2-δ functions PDF, and Clipped-Gaussian PDF for 86 M/S Fuel Mean Velocity, 1% Inlet Fuel Stream Turbulence

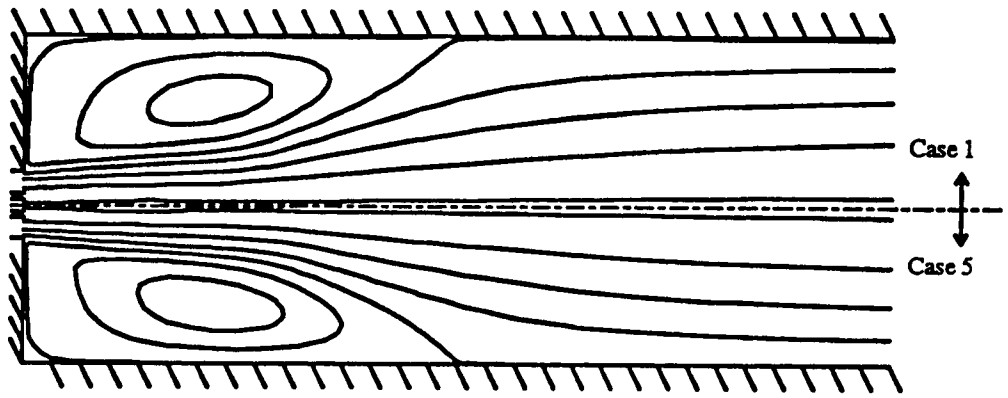

(a) 2-δ functions pdf

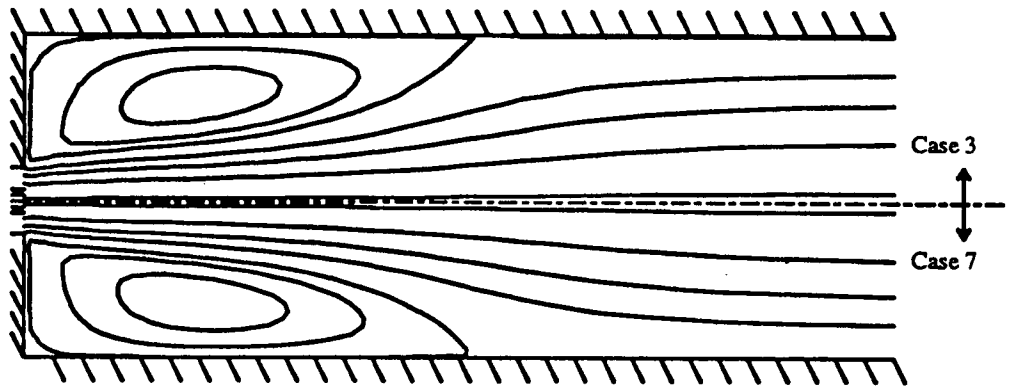

(b) Clipped Gaussian pdf

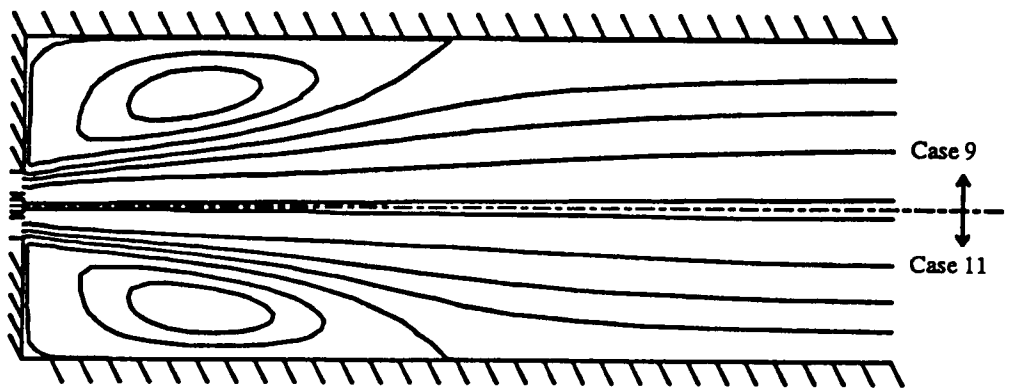

(c) No pdf

Figure 8. Comparison of Recirculation Zone Structure for Changes in Fuel Mean Velocity (7 & 25 m/s), 1% Inlet Fuel Stream Turbulence

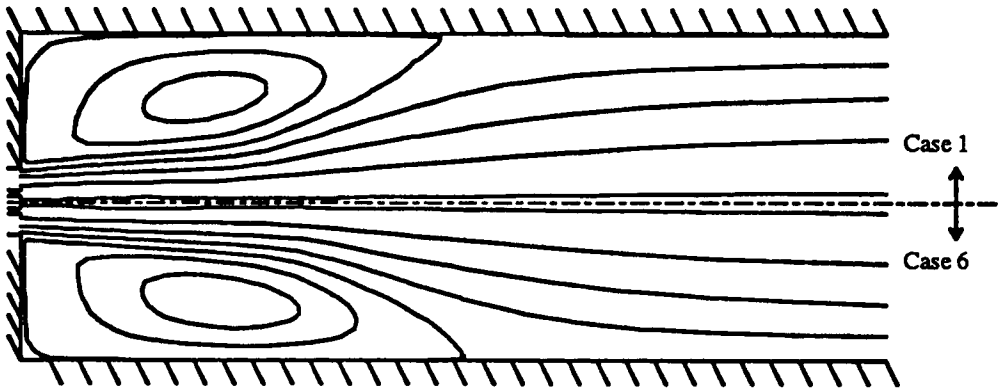

(a) 2-δ functions pdf

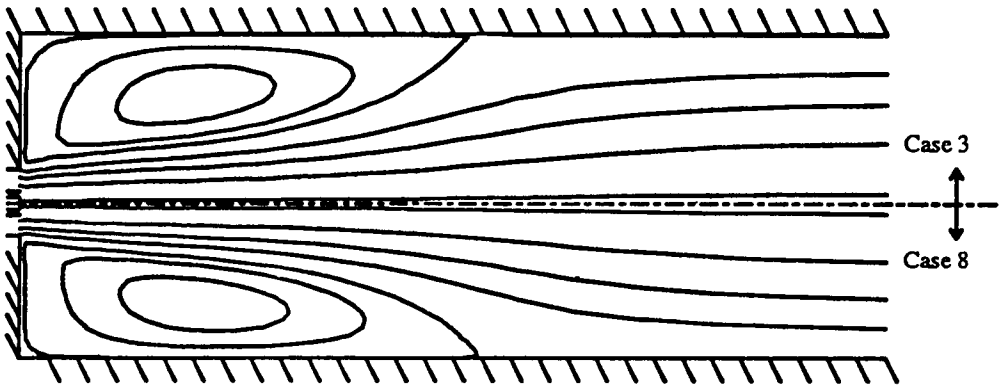

(b) Clipped Gaussian pdf

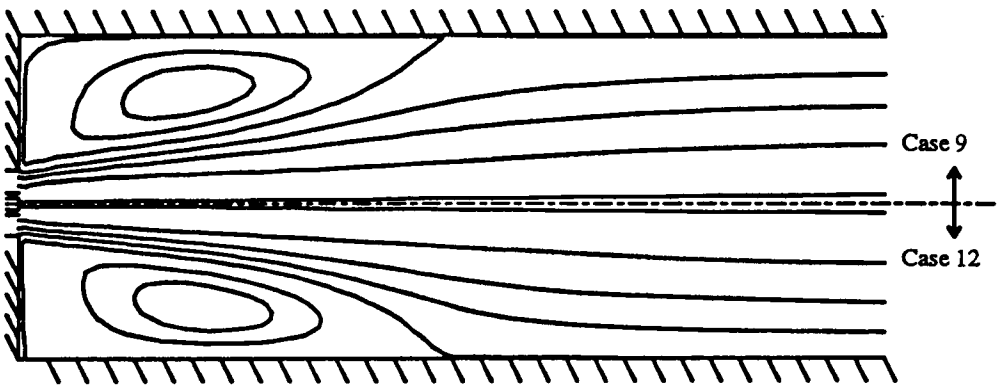

(c) No pdf

Figure 9. Comparison of Recirculation Zone Structure for Changes in Fuel Mean Velocity (7 & 86 m/s), 1% Inlet Fuel Stream Turbulence

inlet fuel mean velocity. They retained virtually the same volume, and had the same reattachment (or rear stagnation) point. For the two-delta function pdf, and Clipped-Gaussian pdf, the recirculation zone grew slightly as the inlet fuel velocity was increased.

Figure 10 shows the comparisons of recirculation zones between three methods with the inlet fuel stream turbulent intensity level at 5%. The structure in each calculation (10a, 10b, and 10c) shows that increasing fuel stream turbulence from 1 to 5% had an insignificant effect on the computed solutions.

Figure 11 shows the same results wherein the calculations are compared for each method at 1% and 5% turbulence levels. One can see that almost nothing changed in streamline geometry for each method when increasing the inlet fuel stream turbulent intensity level from 1% to 5%. In order to see just how insensitive the solutions were to the inlet fuel stream turbulence level, three cases were computed with 25% inlet turbulence. It was expected that some significant structure features of the flow would change. But, when increasing the inlet fuel stream turbulent intensity level from 1% to 25%, as shown in Fig. 12, the recirculation zones increase only very slightly in size for the 2-δ function pdf model. For the Clipped-Gaussian case, the difference is a small increase in volume. For no pdf, the changes were insignificant.

So the comparison of the streamline patterns, recirculation zone centers, and separating streamline reattachment points on the wall showed few and relatively small differences for all 15 cases. None of the differences noted were thought to be significant in comparison for diagnostic purposes. That is, the appearance of

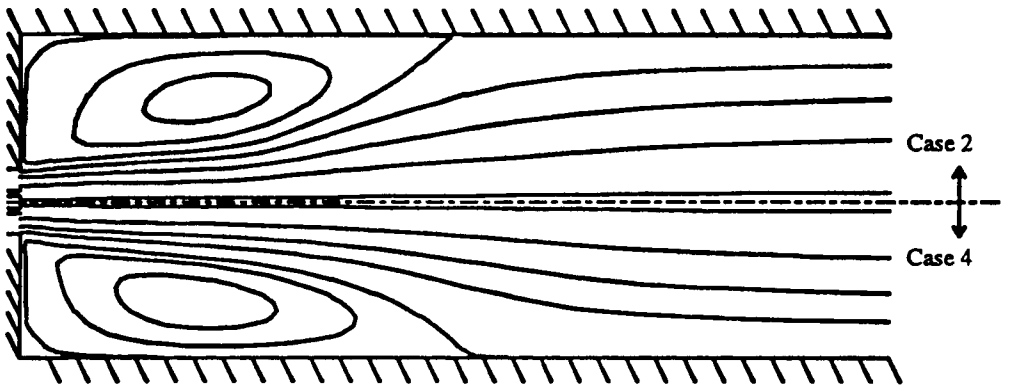

(a) 2-δ functions pdf versus Clipped Gaussian pdf

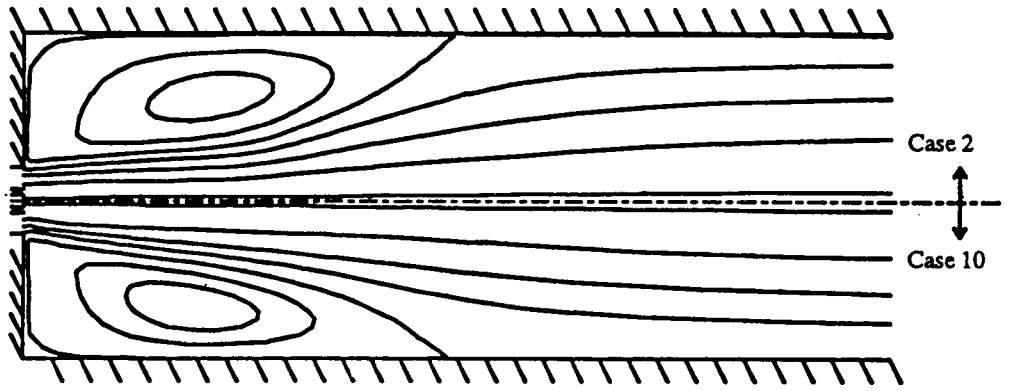

(b) 2-δ functions pdf versus No pdf

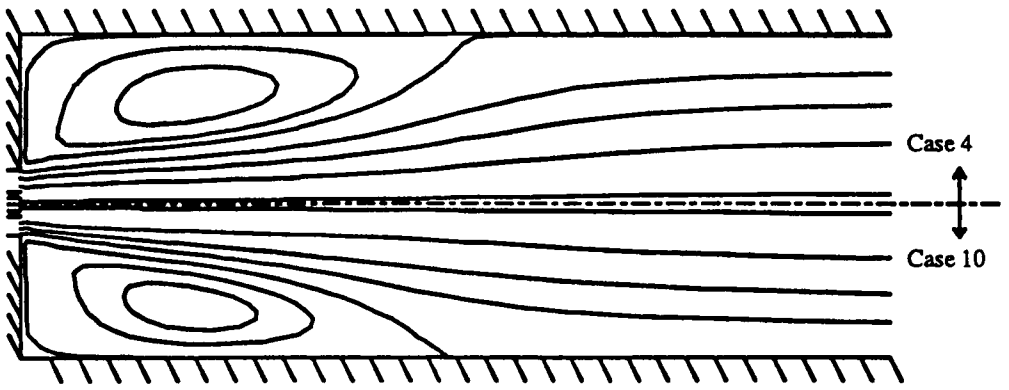

(c) Clipped Gaussian pdf versus No pdf

Figure 10. Comparison of Recirculation Zone Structure Obtained with No-pdf, 2-δ functions PDF, and Clipped-Gaussian PDF for 5% Fuel Turbulence Intensity, 7 m/sec Inlet Fuel Mean Velocity

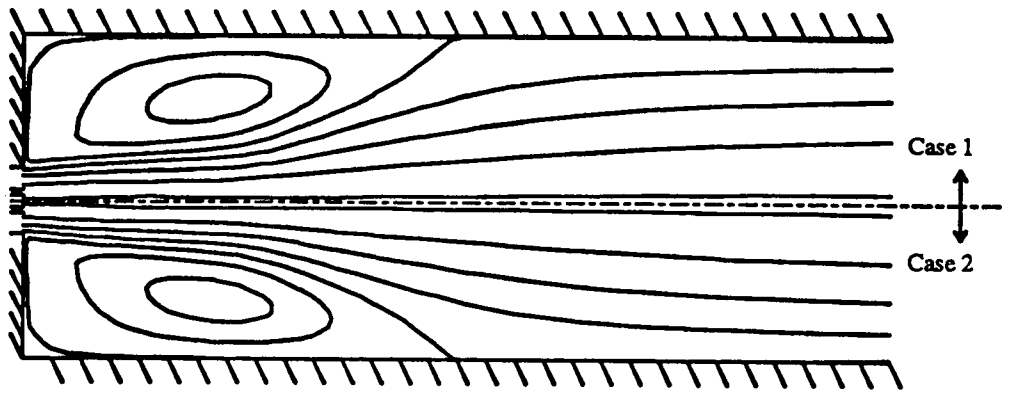

(a) 2-δ functions pdf, 1% and 5% Inlet Fuel Stream Turbulence

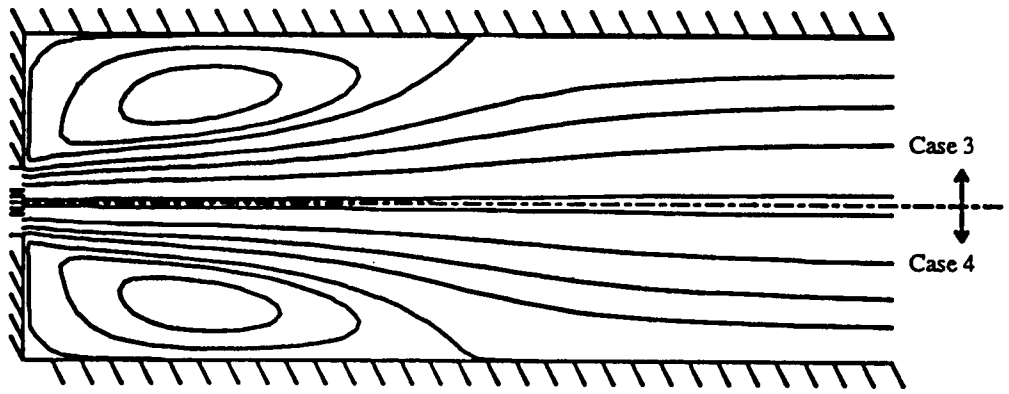

(b) Clipped Gaussian pdf, 1% and 5% Inlet Fuel Stream Turbulence

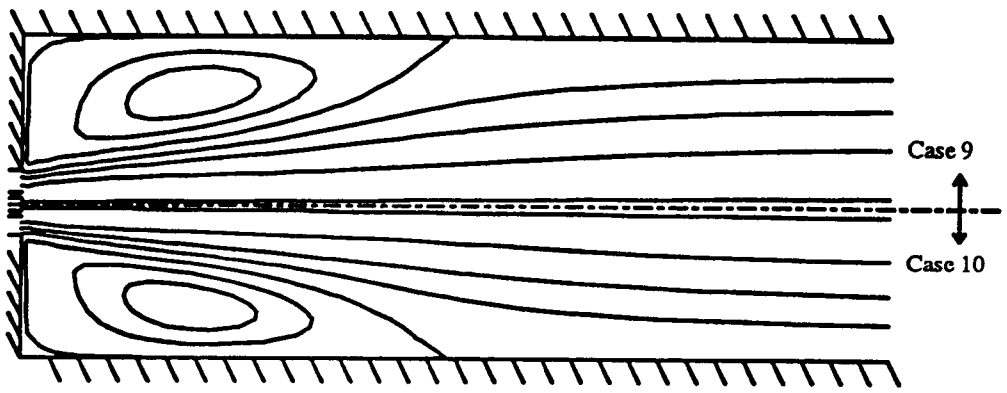

(c) No pdf, 1% and 5% Inlet Fuel Stream Turbulence

Figure 11. Comparison of Recirculation Zone Structure for Changes in Turbulence Intensity, 7 m/sec Inlet Fuel Mean Velocity

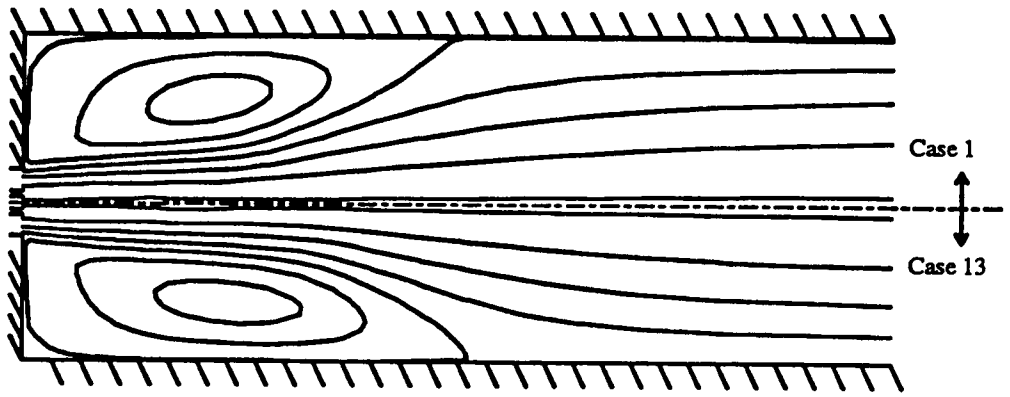

(a) 2-δ functions pdf, 1% and 25% Inlet Fuel Stream Turbulence

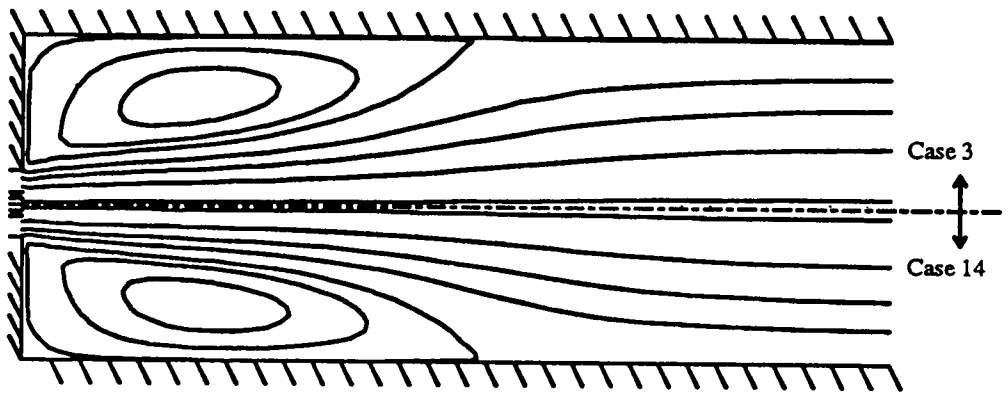

(b) Clipped Gaussian pdf, 1% and 25% Inlet Fuel Stream Turbulence

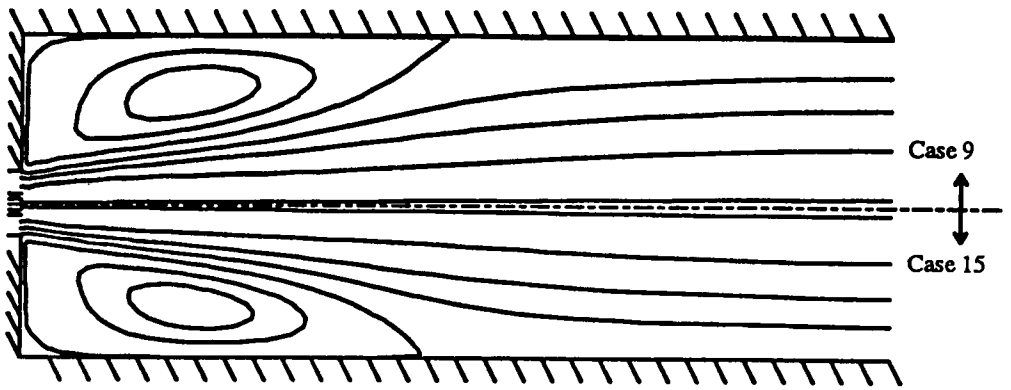

(c) No pdf, 1% and 25% Inlet Fuel Stream Turbulence

Figure 12. Comparison of Recirculation Zone Structure for Changes in Turbulence Intensity, 7 m/sec Inlet Fuel Mean Velocity

the computed mean streamline patterns in the combustor could not be used to estimate the velocity levels, the turbulence levels, or whether or not a pdf was used, in the calculation of the internal flows fields.

4.2.2. Profiles of Mean Scalar Quantities

The profiles of several of the predicted mean scalar flow quantities across the combustor were plotted for comparison at different axial distances downstream of the combustor inlet. To simplify the comparison of the results, and to provide the greatest generality, the results from Cases 1, 3, and 9 are compared first. Case 1 corresponds to the two-delta function pdf, Case 5 to the Clipped-Gaussian pdf, and Case 9 to no pdf. For these cases, the mean fuel velocity was 7 m/s and the fuel stream turbulence intensity was 1%.

Figure 13 shows the profiles of mean axial velocity (m/s); Fig. 14 shows profiles of mean temperature (K); Fig. 15 shows profiles of mean density (kg/m^3); Fig. 16 shows profiles of turbulent kinetic energy ($(m/s)^2$); Fig. 17 Shows profiles of effective turbulent viscosity ($kg/m-s$).

Figure 13 shows that the calculations without a pdf have a greater axial velocity on the centerline and at the location of peak temperature than either pdf case. This is interpreted to mean that the pdf models predict greater mixing and thus shear. The two-delta function pdf lead to greatest mixing and the largest rate of decay of centerline velocity from inlet to outlet. The Clipped-Gaussian results in the next faster mixing rate. Finally, the case of no pdf leads to the smallest mixing rate.

Figure 14 shows the mean temperature profiles and it is clear that the no-pdf Case produces a very narrow and high temperature zone, where as both pdf

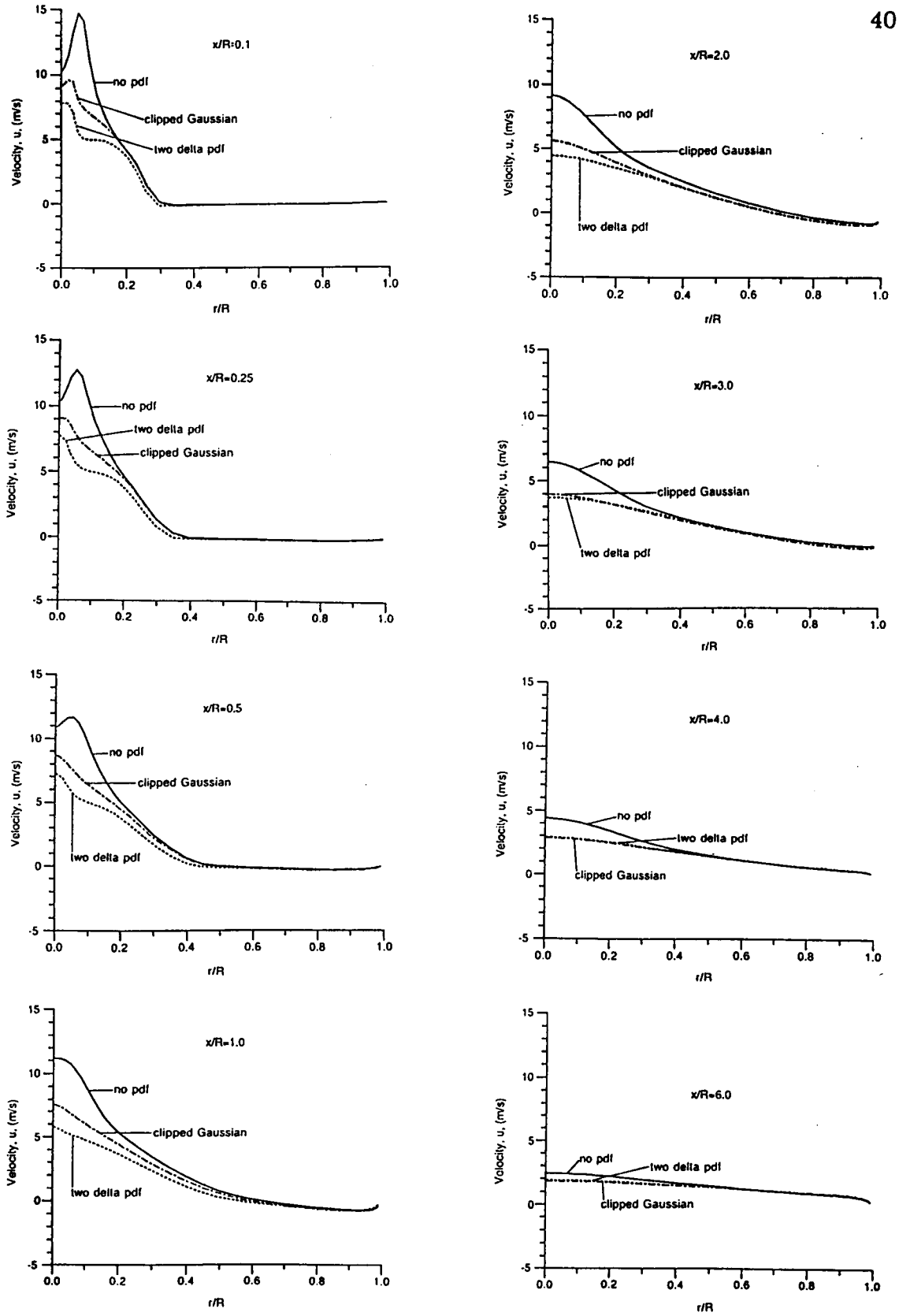

Figure 13. Comparison of Predicted Mean Axial Velocity Profiles Across Combustor

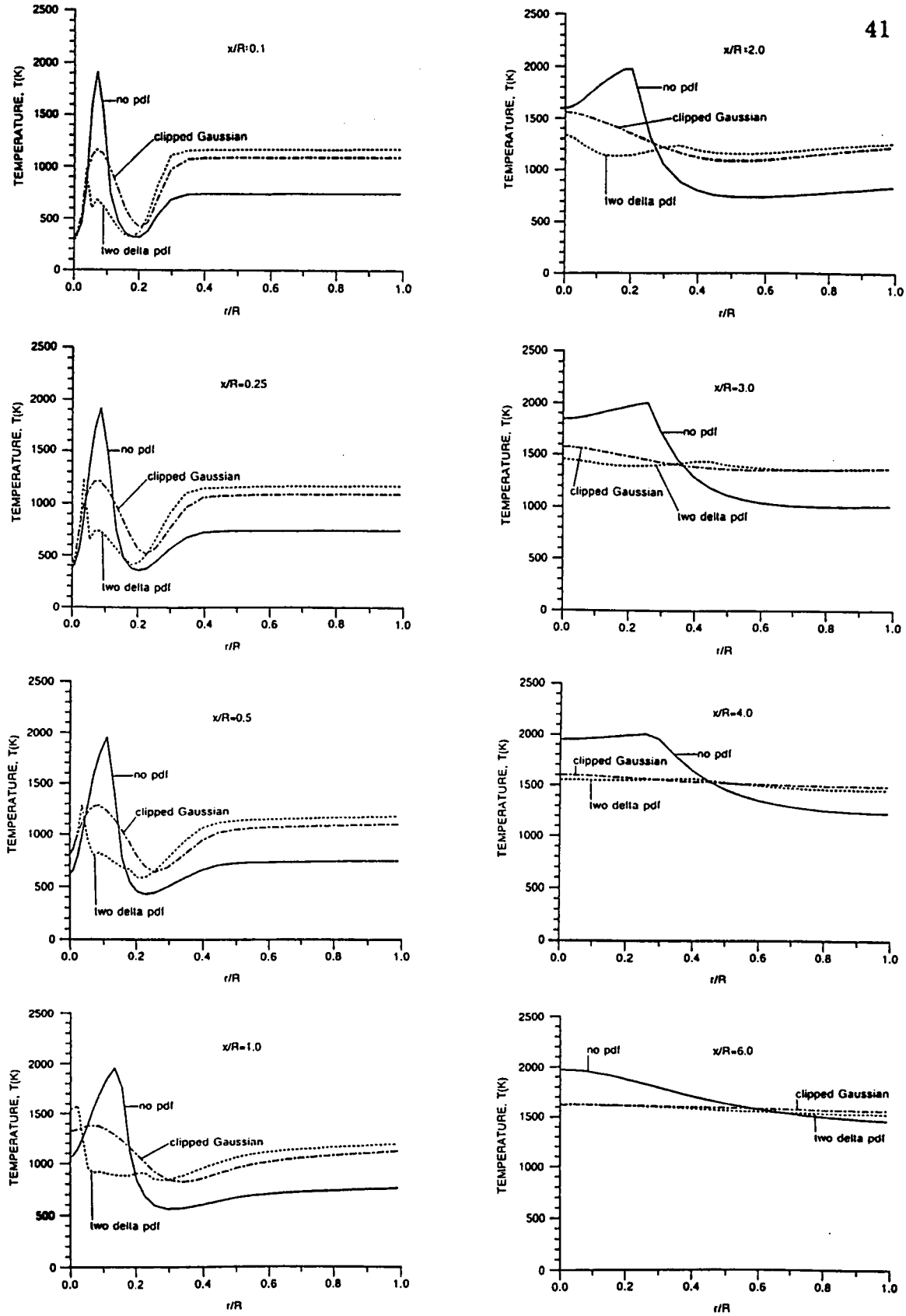

Figure 14. Comparison of Predicted Mean Temperature Profiles Across Combustor

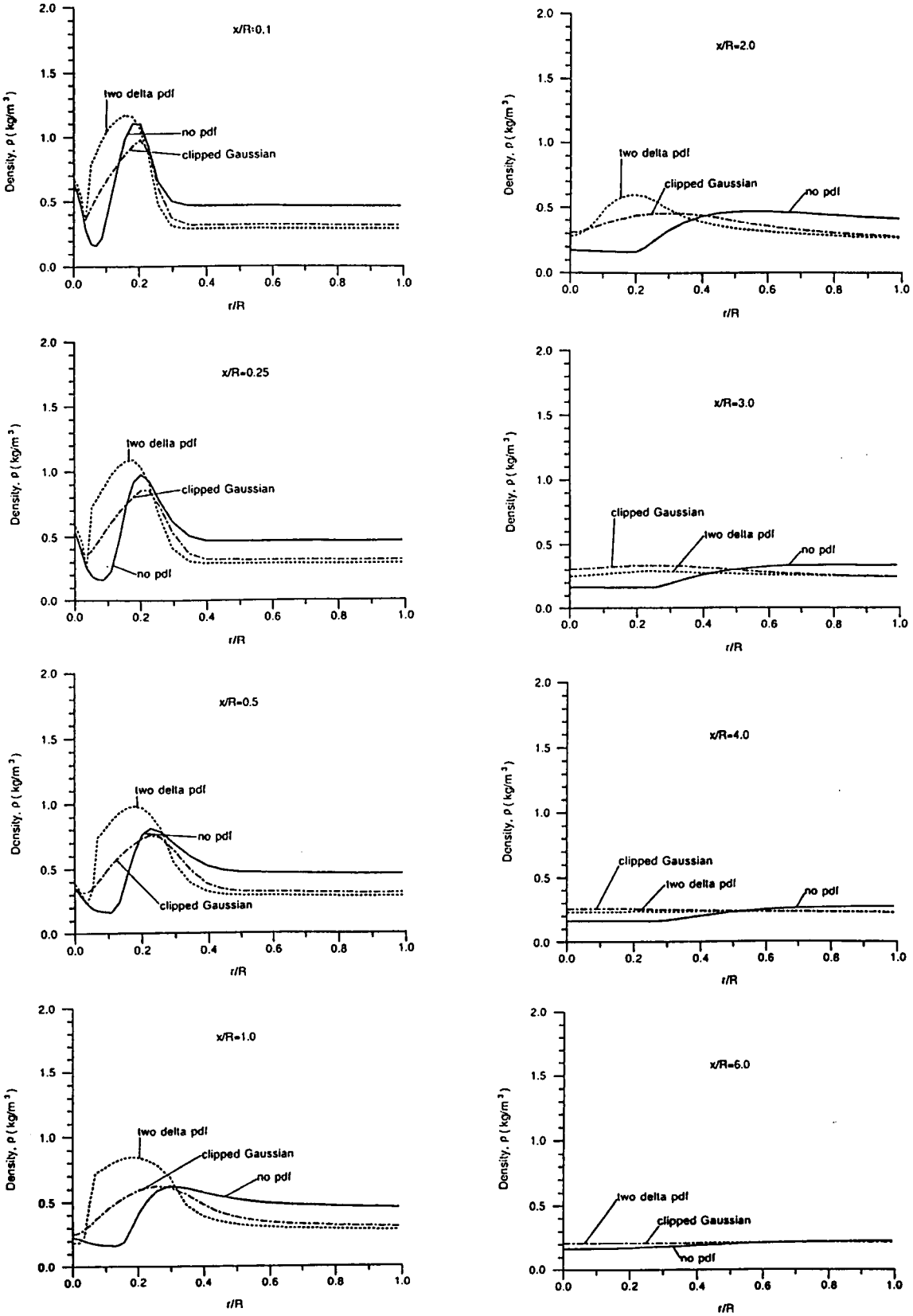

Figure 15. Comparison of Predicted Mean Density Profiles Across Combustor

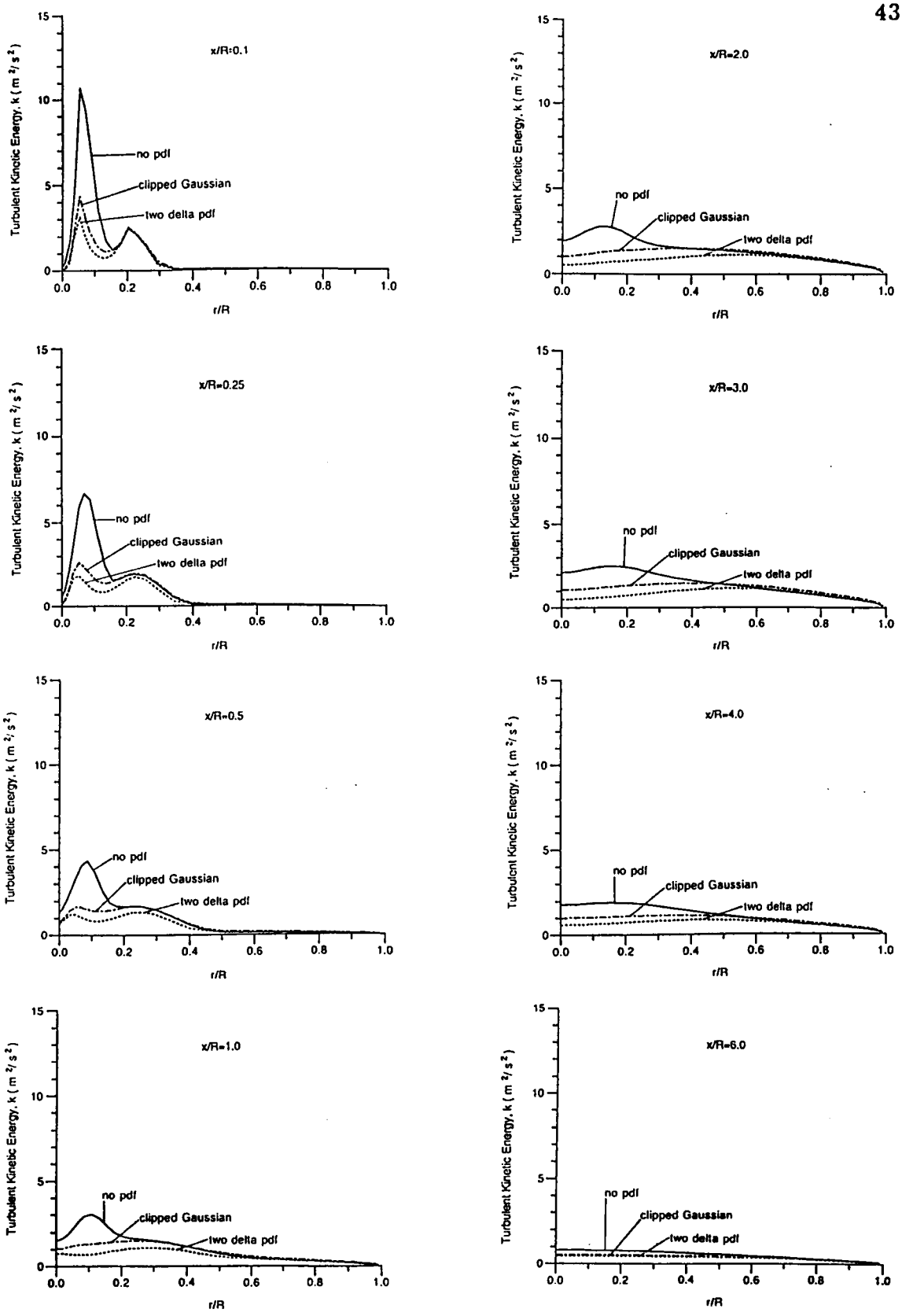

Figure 16. Comparison of Predicted Mean Turbulent Kinetic Energy Profiles Across Combustor

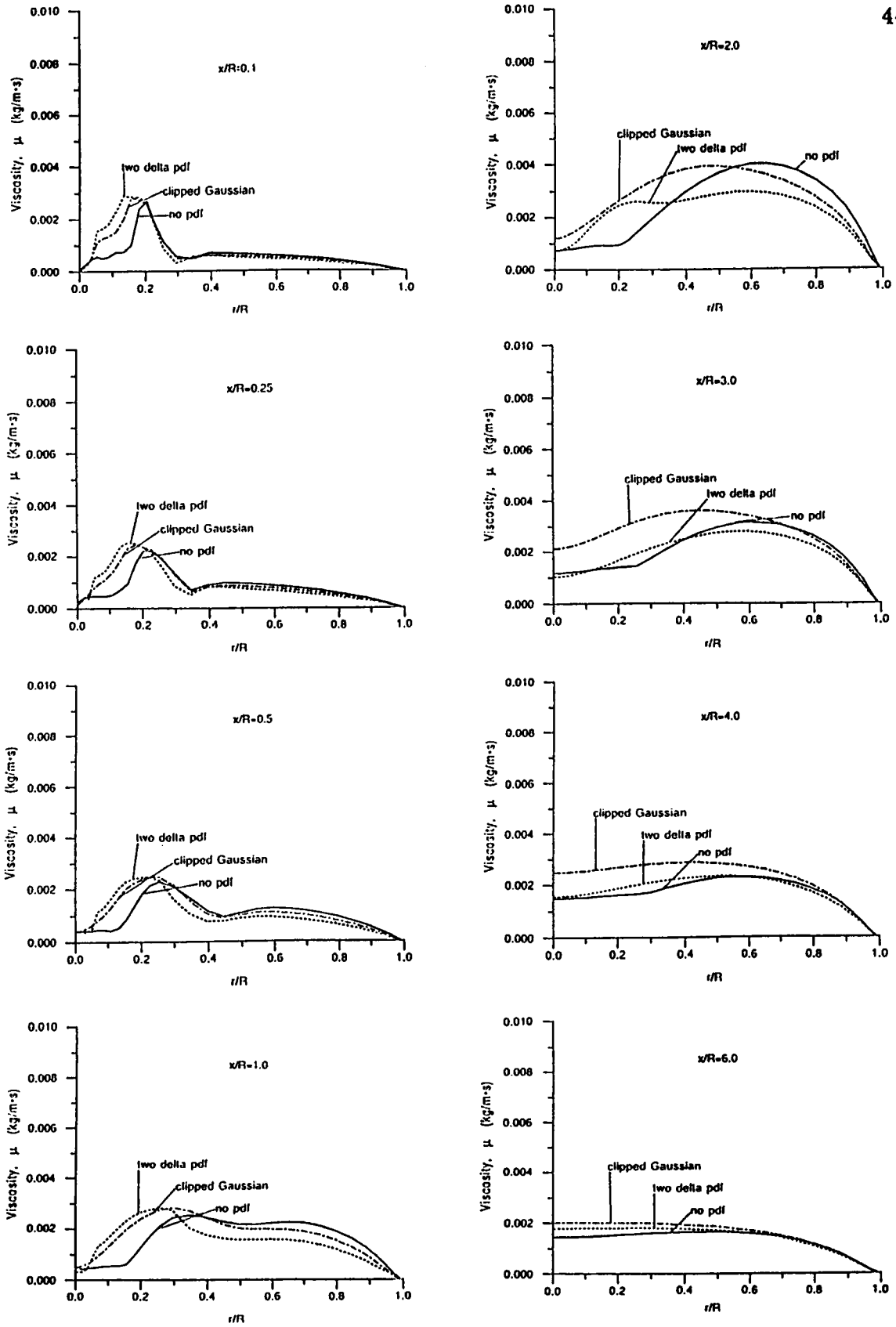

Figure 17. Comparison of Predicted Mean Turbulent Effective Viscosity Profiles Across Combustor

functions create a much more diffuse temperature field. Also, because of "turbulence" (acting through the transport of g), the pdf models predict a higher temperature out in the recirculation zone and near the wall. The two-delta function pdf causes a narrow high temperature flame, compared to the Clipped-Gaussian, in the near field, but both pdf Cases predict a much lower peak flame temperature about 1400-1500 ^{0}K, compared to about 2000 ^{0}K for the no pdf case. Note that the pdf methods yield a temperature twice as high as the no pdf case out in the recirculation zone near the wall. This effect is rather remarkable. Interestingly, Khalil [6] provides experimental data (Appendix in Khalil [6]) that shows this effect physically. The implications of this could be very significant for the analysis of heat transfer and combustion chemistry in recirculating flow combustors. However, the study of these implications is beyond the scope of the present study. In this study, however, just to check that $\bar{f}$ (and, hence, total enthalpy) was being conserved, integrals of the flux of $\bar{f}$ were computed as

$$I_f(x) = 2\pi \int_0^{R_w} \rho u \bar{f} r dr \Big|_x \tag{4.1}$$

It was found that $I_f(x)$ was constant, within a 5 percent variation, at most, from inlet to outlet for the various cases. Thus, the high temperatures in the recirculation zones predicted with the pdf methods appears to be a result of the approach and not a numerical error. Further, as Khalil's presentation shows, there may be experimental evidence for such temperature profiles.

Figure 15 shows the mean density profiles for these cases, and, as expected the high flame temperature regions of all the flames yield the lowest density regions. Note that all the cases predict that an annular, highest density zone occurs on the air-side of the flame sheet, and that this density is greater than the density in the outer recirculation zones. This is due to the molecular weight and temperature

distributions obtained, as Fig. 14 shows.

Figure 16 shows the profiles of turbulent kinetic energy. They are bi-modal in the near field. These shapes result from the shear-driven production of turbulence on the inner, fuel-rich side of the flame zone, and also on the air jet outer shear layer, that drives the outer recirculation zone. The no-pdf case generated the highest levels of turbulent kinetic energy, which might lead one to think that the no-pdf case would result in the fastest turbulent mixing being predicted. However, temperature effects cause the no-pdf case to have the lowest density in the high k regions. Thus, the parameter to examine that explains the mixing results is the distribution of turbulent effective viscosity.

Figure 17 shows the turbulent effective viscosity (μ_E) distributions for these cases. These profiles appear fairly similar in shape and magnitude, even with the large differences in temperature, density, and turbulent kinetic energy between the three cases. The profiles show that the two-delta function and Clipped-Gaussian pdf methods resulted in the highest levels of turbulent viscosity, in the flow near the inlet. The no pdf calculation provided slightly higher μ_E near the walls than either pdf method. These results were interpreted to imply that the pdf methods yield the faster mixing rates, and that the very slightly different recirculation zone structure that obtained with these methods were attributable to fairly similar effective viscosity distributions.

The flow mean velocity at the walls was very low, and the wall-functions did not predict significant levels of turbulent kinetic energy or effective viscosity in these regions of the flow. Smaller diameter combustor geometries might create significantly different results out near the walls by causing higher mean (reverse-flow) velocities. Further study should investigate such effects.

CHAPTER V

SUMMARY AND CONCLUSIONS

5.1. Summary

In summary, a numerical sensitivity study was performed of a single combustor flow modeled in three ways. Given a flame-sheet model for the turbulent flame, the flow was computed with the same mesh, turbulence transport model, boundary conditions, and inlet conditions with:

(1) No-pdf

(2) Two-delta function pdf

(3) Clipped-Gaussian pdf

in order to relate mean temperature and density distributions to the predicted mean fuel-fraction distributions. The purpose of the study was to determine the sensitivity of the predicted flow, in terms of both quality and quantity, to the use, or not, of pdf functions, and then, to variations in the mean velocity and turbulence intensity of the fuel jet entering the combustor, for constant fuel/air ratio.

5.2. Conclusions

The results showed that the case of no-pdf generated the highest flame temperatures, the lowest density and the lowest rate of mixing (in the near field about the flame sheet) than either the two-delta function method or the Clipped-Gaussian method. Of the methods, the Clipped-Gaussian produced the most diffuse temperature and density fields. Both pdf methods yielded predicted flows with significantly lower peak flame temperatures than the no pdf method (i.e. 1500 K

vs 2000 K). However, the pdf methods produced recirculation zone temperatures twice as high as that obtained without a pdf approach (i.e. 1100 K vs 600 K).

This kind of temperature behavior has been reported experimentally. Thus, engineering calculations of recirculating combustor flow may require a pdf approach for accurate simulation.

Finally, although a detailed comparison was not presented in the paper, the predicted flow field was sensitive to the input fuel mean-velocity (Reynolds number effects) or its turbulence intensity level. The largest differences were due to the use, or not, of a pdf method, and, to the pdf actually implemented.

In summary, the present study supports the use of pdf functions in application to the practical prediction of recirculating combustor flows because of the significantly different qualitative and quantitative aspects of the predictions, which apparently are realistic.

LIST OF REFERENCES

LIST OF REFERENCES

1. Kuo, Kenneth K. "Principles of Combustion" (John Wiley & Sons, Inc.), 1986.
2. Williams, F. A. "Combustion Theory" (Addison-Wesley, Reading, Mass.), 1965.
3. Bilger, R. W. and Kent, J. H. "Measurements in Turbulent Diffusion Flames." Sydney University, Dept. of Mechanical Engineering, Report F41, 1972.
4. El Ghobashi, S. E. "Characteristics of Gaseous Turbulent Diffusion Flames in Cylindrical Chambers, a Theoretical and Experimental Investigation." Ph.D. Thesis, London University, 1974.
5. Spalding, D. B. "Concentration Fluctuations in a Round Turbulent Free Jet," Chem. Eng. Sci., Vol. 26, p. 95, 1971.
6. Khalil, E. E. Modeling of Furnaces and Combustors, Abacus Press, 1982.
7. Naguib, A. S. "The Prediction of Axisymmetric Free Jet, Turbulent Reacting Flows." Ph.D. Thesis, London University, 1975.
8. Patankar, Suhas V. "Numerical Heat Transfer and Fluid Flow "Hemisphere Publishing Corporation, 1980.
9. Pope, S. B. "PDF Methods for Turbulent Reactive Flows,"Progress in Energy and Combustion Science, Vol. 11, No. 2, pp 119, 1985
10. Jones, W. P., and Whitelaw, J. H. "Calculation Methods for Reacting Turbulent Flows,"paper in Predication of Turbulent Reacting Flows in Practical Systems, presented at The Fluids Engineering Conference, Bouldes, Colorado, June 22-24, 1981, edited by T. Morel, The American Society of Mechanical Engineers.

11. Libby, P. A., and Williams, F. A. editors Turbulent Reacting Flows, Topics in Applied Physics, Volume 44, Springes-Verlag, 1980.

12. Damkohler, G. Z. (1974) "On the Effect of Turbulence on the Flame Velocity in Gas Mixtures," NACA, T.M. 1112.

13. Bilger, R. W. "Turbulent Flows with Non-premixed Reactants," Turbulent Reacting Flows(P. A. Libby and F. A. Williams, Eds.), Chapter 3, pp. 65-114, Topics in Applied Physics, Springer-Verlag, New York, 1980.

14. Burke, S. P., and Schumann, T. E. W. "Diffusion Flames," Industrial and Engineering Chemistry, 20,pp 998, 1928.

15. Emmons, H. W. "The Film Combustion of Liquid Fuel" Z. angew. Math. Mech. Bd. 36 Nr. 1/2 Jan./Feb., 1956.

16. El Ghobashi, S. E. and Pun, W. M. "A Theoretical and Experiment Study of Turbulent Diffusion Flames in Cylindrical Furnaces" Proc. 15th Symp. (Int.) on Combustion, p. 1353, 1974.

17. Khalil, E. E., Spalding, D. B., and Whitelaw, J. H. "The Calculation of Local Flow Properties in Two-Dimensional Furnaces,"Int. J. Heat Mass Transfer, Vol. 18, p. 775, 1975.

18. Richter, W. Ph.D Dissertation, University of Stuttgart

19. Gosman, A. D. and Lockwood, F. C., "Prediction of the Influence of Turbulent Fluctuations on Flow and Heat Transfer in Furnaces," Proc. Heat Mass Transfer Seminar, Int. Summer School, Trogir, Yugoslavia, Vol. 4, p. 215, 1973.

20. Kent J. H. and Bilger, R. W. "Turbulent Diffusion Flames,"Report 7N F-37, University of Sydney; see also 14th Symposium in Combustion, p. 615, 1973.

21. Jones, W. P. "Models for Turbulent Flows with Variable Density," VKI Lecture Series 1979-2, Prediction Methods for Turbulent Flows (W. Kollmann, Ed.), Hemisphere Publ. Corp., New York, 1980.

22. Lockwood, F. C. and Bilger, R.W. "The Prediction of Fluctuations in the Properties of Free, Round-Jet, Turbulent, Diffusion Flame," Combustion and Flame, Vol. 24, pp. 109-124.

23. Kent, J. H. and Bilger, R. W. "The Prediction of Turbulent Diffusion Flame Fields and Nitric Oxide Formation," 16th Symposium (Int.) on Combustion, pp. 1643-1656, 1977.

24. Shearer, A. J. "Evaluation of a locally homogeneous flow model of spray evaporation,"Ph.D. Thesis, 1980, Pennsylvania State

25. Lilley, D. G., and Rhode, D. L. "A Computer Code for Swirling Turbulent Axisymmetric Recirculating Flows in Practical Isothermal Combustor Geometries" Report NASA Cr-3442, Feb., 1982.

26. Samples, J. W. "Prediction of Axisymmetric Chemically-Reacting Combustor Flow Fields,"Ph.D. Dissertation, Oklahoma State University, May, 1983.

27. Launder, B. E. "Progress in Modeling of Turbulent Transport," Lecture Series 76, von Karman Institute for Fluid Dynamics, Belgium, 1975.

28. Launder, B. E. and Spalding, D. B."The Numerical Computation of Turbulent Flows," Computer Method Appl. Mech. Engrg., Vol. 3, p.,239, 1974.

29. Wilox, D. C. and Traci, R. M."A Complete Model of Turbulence" AIAA, Fluid and Plasma Dynamics Conference, 7th, Palo Alto, Calif., June 17-19, 1974.

APPENDIXES

APPENDIX A

DERIVATION OF 2-DELTA FUNCTION PDF

Define

$$f_- = \bar{f} - \sqrt{g} \tag{A.1}$$

$$f_+ = \bar{f} + \sqrt{g} \tag{A.2}$$

and define the $\delta(\ )$ function as follows:

$$\delta(f) = \begin{cases} 1 & \text{if} \quad f = 0 \\ 0 & \text{if} \quad f \neq 0 \end{cases} \tag{A.3}$$

Since

$$\int_0^1 p(f)df = 1 \tag{A.4}$$

we have

$$\begin{aligned} \int_0^1 p(f)df &= \int_0^1 [\alpha_1 \delta(f - f_-) + \alpha_2 \delta(f - f_+)]df \\ &= \alpha_1 + \alpha_2 \end{aligned}$$

So

$$\alpha_1 = 1 - \alpha_2$$

Therefore, define

$$\alpha \equiv \alpha_1 = 1 - \alpha_2 \tag{A.5}$$

Hence, we can write

$$p(f) = \alpha \cdot \delta(f - f_-) + (1 - \alpha)\delta(f - f_+). \tag{A.6}$$

For $f_- > 0$ and $f_+ < 1$, we have

$$\begin{aligned} \bar{f} &= \int_0^1 f p(f)df \\ &= \int_0^1 f\alpha\delta(f - f_-) + \int_0^1 f(1 - \alpha)\delta(f - f_+)df \\ &= \alpha f_- + (1 - \alpha)f_+ \end{aligned} \tag{A.7}$$

where the constant α is arbitrary, a freely selectable constant that can range from 0 to 1. In the present model, $\alpha = 0.5$, which was suggested by Spalding as repeated by Khalil [6].

However, when f_- and f_+ are calculated from eq. (A.1) and (A.2) such that $f_- < 0$, and/or $f_+ > 1$ then the constant α must be determined by setting $f_- = 0$ and $f_+ = 1$.

For $f_- < 0$ and $f_+ < 1$, let $f_- = 0$, then

$$p(f) = \alpha \cdot \delta(f) + (1 - \alpha)\delta(f - f_+) \tag{A.8}$$

therefore since

$$\begin{aligned}
\bar{f} &= \int_0^1 f p(f) df \\
&= \int_0^1 f \alpha \delta(f) df + \int_0^1 f(1 - \alpha)\delta(f - f_+) df \\
&= 0 + (1 - \alpha) f_+ \\
&= \bar{f} + \sqrt{g} - \alpha(\bar{f} + \sqrt{g})
\end{aligned}$$

then

$$\alpha = \frac{\sqrt{g}}{\bar{f} + \sqrt{g}} \tag{A.9}$$

Alternately when $f_+ > 1$ and $f_- > 0$, let $f_+ = 1$, then

$$p(f) = \alpha\delta(f - f_-) + (1 - \alpha)\delta(f - 1) \tag{A.10}$$

then write

$$\begin{aligned}
\bar{f} &= \int_0^1 f p(f) df \\
&= \int_0^1 f \alpha \delta(f - f_-) df + \int_0^1 f(1 - \alpha)\delta(f - 1) df \\
&= \alpha f_- + (1 - \alpha) \\
&= 1 - \alpha(1 - f_-) \\
&= 1 - \alpha(1 - \bar{f} + \sqrt{g})
\end{aligned}$$

Solving for α,

$$\alpha = \frac{1 - \bar{f}}{1 - \bar{f} + \sqrt{g}}. \tag{A.11}$$

APPENDIX B

INLET CONDITION FOR MEAN AXIAL VELOCITY

For the annular air stream, the distribution of axial velocity is

$$u = \begin{cases} u_{max}\left(\frac{r - R_F}{\delta}\right)^{\frac{1}{\eta}} & \text{if} \quad R_F < r < R_F + \delta \\ u_{max} & \text{if} \quad R_F + \delta < r \leq R_A - \delta \\ u_{max}\left(\frac{R_A - r}{\delta}\right)^{\frac{1}{\eta}} & \text{if} \quad R_A - \delta < r \leq R_A \end{cases} \tag{B.1}$$

then the average axial inlet velocity is,

$$\begin{aligned} U_{A_0} &= \int_{R_F}^{R_A} u \frac{2\pi r dr}{\pi(R_A^2 - R_F^2)} \\ &= \frac{2}{R_A^2 - R_F^2}\left[\int_{R_F}^{R_F+\delta} u_{max}\left(\frac{r - R_F}{\delta}\right)^{1/\eta} r dr + \int_{R_F+\delta}^{R_A-\delta} u_{max} r dr \right. \\ &\qquad \left. + \int_{R_A-\delta}^{R_A} u_{max}\left(\frac{R_A - r}{\delta}\right)^{1/\eta} r dr\right] \\ &= \frac{2u_{max}}{R_A^2 - R_F^2}[I_1 + I_2 + I_3] \end{aligned}$$

where

$$I_1 \equiv \int_{R_F}^{R_F+\delta} r\left(\frac{r - R_F}{\delta}\right)^{1/\eta} r dr \tag{B.2}$$

Let $y = (r - R_F)/\delta$, then we get

$$\begin{aligned} I_1 &= \delta^2\left[\int_0^1 y^{1+\frac{1}{\eta}} dy + \int_0^1 \frac{R_F}{\delta} y^{\frac{1}{\eta}} dy\right. \\ &= \frac{\delta^2}{2 + \frac{1}{\eta}} + \frac{\delta R_F}{1 + \frac{1}{\eta}} \end{aligned} \tag{B.3}$$

$$\begin{aligned} I_2 &\equiv \int_{R_F+\delta}^{R_A-\delta} r dr \\ &= \frac{1}{2}[(R_A - \delta)^2 - (R_F + \delta)^2] \\ &= \frac{1}{2}(R_A + R_F)(R_A - R_F - 2\delta) \end{aligned} \tag{B.4}$$

$$I_3 \equiv \int_{R_A-\delta}^{R_A} \left(\frac{R_A - r}{\delta}\right)^{1/\eta} r\,dr \tag{B.5}$$

Let $y = (R_A - r)/\delta$, then

$$\begin{aligned} I_3 &= \delta^2 \left[\int_0^1 \frac{R_A}{\delta} y^{\frac{1}{\eta}} dy - \int_0^1 t^{1+\frac{1}{\eta}} dy \right] \\ &= \frac{\delta R_A}{1+\frac{1}{\eta}} - \frac{\delta^2}{2+\frac{1}{\eta}} \end{aligned} \tag{B.6}$$

So,

$$\begin{aligned} U_{A_0} &= \frac{2u_{max}}{R_A^2 - R_F^2} \left(\frac{\delta^2}{2+\frac{1}{\eta}} + \frac{\delta R_F}{1+\frac{1}{\eta}} + \frac{1}{2}(R_A + R_F)(R_A - R_F - 2\delta) \right. \\ &\qquad \left. + \frac{\delta R_A}{1+\frac{1}{\eta}} - \frac{\delta^2}{2+\frac{1}{\eta}} \right) \\ &= u_{max} \left[1 - \frac{2\delta}{1+\eta} \frac{1}{R_A - R_F} \right] \end{aligned} \tag{B.7}$$

or

$$u_{max} = \frac{U_{A_0}}{1 - \frac{2\delta}{1+\eta} \frac{1}{R_A - R_F}} \tag{B.8}$$

VITA

Xiaohang Peng was born in Tianjing, China on November 10, 1959. He received his elementary and high school education in Beijing, China. In July 1982 he graduated from the Tsinghua University, Beijing, China, where he received his Bachelor of Science degree with a major in Nuclear Engineering. After graduation, he changed his major to mechanical engineering at Electrical Engineering Institute of the Academia Sinica and earned a Master of Science Degree with a major in mechanical engineering in September, 1985.

In September 1985, he came to The University of Tennessee Space Institute as a graduate research assistant. While working towards the Ph.D., he has received the Master of Science degree in Mechanical Engineering in August, 1988.

He was married to Quan Zhang in August, 1985. They have a daughter Barbara, three months old.